

www.acsaem.org Review

Processing Challenges and Strategies for a Robust Ultrathin Solid Electrolyte Membrane in Sulfide-Based All-Solid-State Batteries

Subin Kim,§ Chaeyeon Shin,§ Jinhan Cho,* and Jieun Lee*



Cite This: ACS Appl. Energy Mater. 2025, 8, 14014-14029



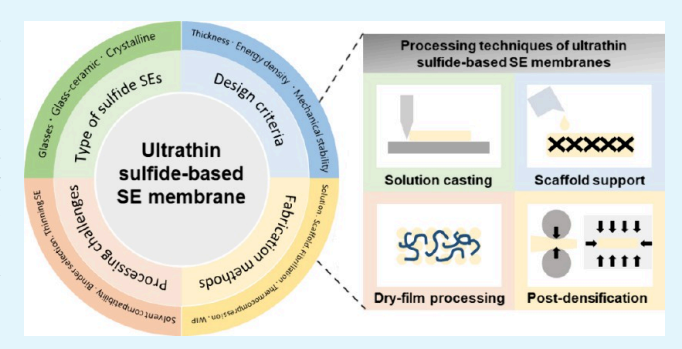
ACCESS

III Metrics & More

Article Recommendations

s Supporting Information

ABSTRACT: All-solid-state batteries (ASSBs) have garnered significant attention as next-generation energy storage systems, offering high theoretical energy density and enhanced safety, and are thus considered as potential replacements for conventional liquid-based lithium-ion batteries (LIBs). Among various solid electrolytes (SEs), sulfide-based SEs are regarded as leading candidates due to their outstanding room-temperature ionic conductivity and excellent processability. Despite their advantages, the fabrication of ultrathin SE membranes remains a critical bottleneck for achieving both high energy density and cost-effective production in practical ASSB systems. In this perspective, we present an overview of the key challenges associated with



ultrathin sulfide-based SE membranes, along with design criteria and recent strategies to address these issues. Particular emphasis is placed on state-of-the-art fabrication techniques, including solution casting, dry film processing, scaffold support, and pressurization-based densification, which enable the formation of ultrathin SE layers. Finally, we provide a perspective on future research directions toward the reliable integration of ultrathin sulfide SE membranes into large-format ASSBs.

KEYWORDS: all-solid-state batteries, sulfide solid electrolytes, binder, membrane fabrication, scalable approach

1. INTRODUCTION

All-solid-state batteries (ASSBs) have attracted significant interest in both academia and industry as a promising next-generation energy storage technology offering enhanced safety. Recent progress in high-capacity anode-free design has boosted the energy density of ASSBs to over 500 Wh kg⁻¹ (gravimetric) and 1100 Wh L⁻¹ (volumetric) (Figure 1a), outperforming conventional liquid-based lithium-ion batteries (LIBs). Furthermore, replacing flammable liquid electrolytes with solid-state counterparts minimizes safety margins and enables a bipolar electrode structure, driving a further increase in energy density at the pack level.

Despite these advantages, numerous challenges remain on the path to ASSB commercialization. To date, research has primarily focused on fundamental studies such as enhancing ionic conductivity, widening the electrochemical stability window of solid electrolytes (SEs), and developing cost-effective synthesis routes. Beyond these material developments, electrode-level manufacturing techniques are crucial for realizing commercially viable ASSBs but have often been overlooked. In particular, greater attention must be directed toward scalable fabrication strategies for producing large-area, sheet-type electrodes and electrolyte films. The electrode manufacturing process for ASSBs generally follows similar steps to those used in conventional LIBs—including mixing composite materials into a homogeneous slurry, casting, drying

or granulating, and subsequently calendering, slitting, and stacking. However, the incorporation of SEs significantly modifies each of these steps. For example, the choice of solvents and binders must ensure chemical compatibility with the SEs. Slurry formulation and rheological properties need to be reoptimized to accommodate higher solid content (SC). Drying protocols must be tailored to the thermal stability of the SE materials. Additionally, compaction processes require further refinement, as precise control of porosity becomes even more critical in the context of ASSBs.

One major difference between ASSBs and conventional LIBs is the insertion of an ultrathin SE membrane between cathode and anode, which functions both as an electronic insulating separator and ion-conducting medium (Figure 1b). The design and fabrication of the SE membrane pose substantial challenges, as multiple property criteria must be met simultaneously. The SE membrane needs to be made as uniform and defect-free across large areas, provide sufficient mechanical strength to prevent lithium dendrite penetration

Received: July 22, 2025
Revised: September 17, 2025
Accepted: September 17, 2025
Published: October 1, 2025





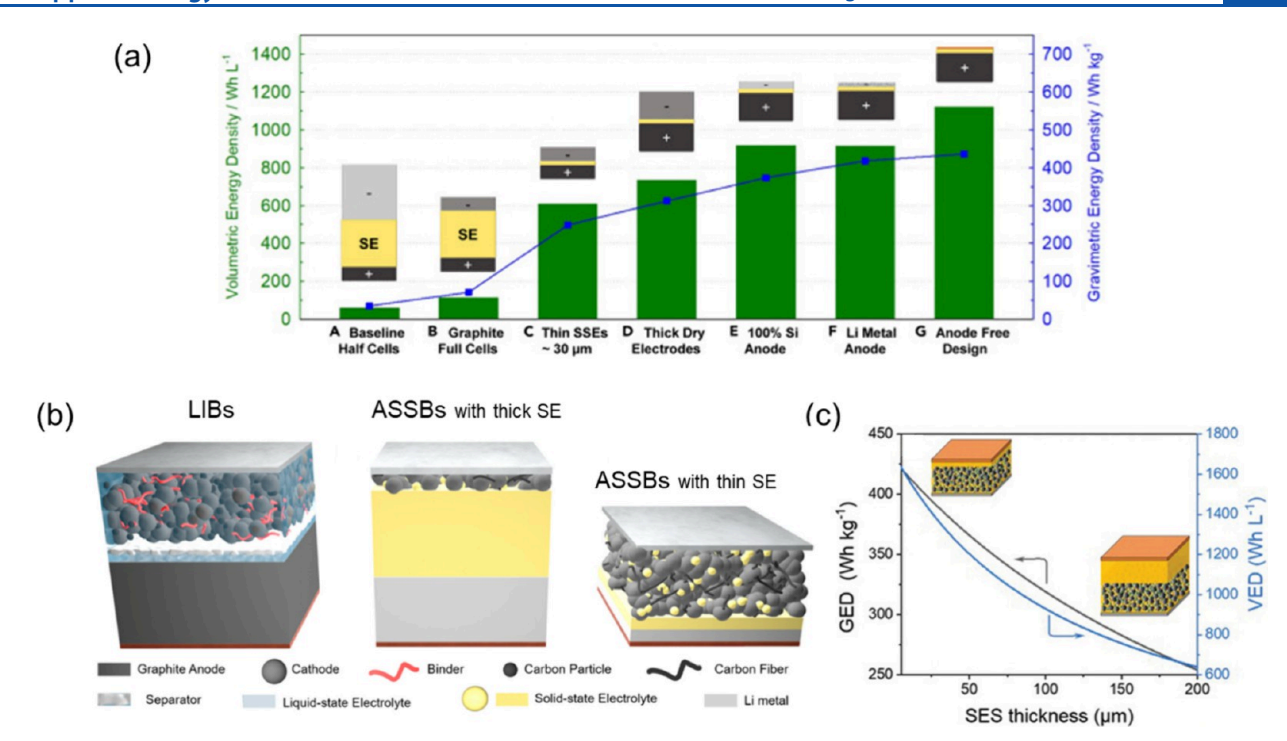


Figure 1. (a) Calculated volumetric and gravimetric energy densities of ASSBs of various cell configurations. Reproduced with permission. Copyright 2022 Cell Press. (b) Schematic cell configuration of conventional LIBs, ASSBs with a thick and thin SE membrane. Reproduced with permission. Copyright 2020 American Chemical Society. (c) Gravimetric (GED) and volumetric (VED) energy densities of ASSB as a function of the solid electrolyte separator (SES) thickness. Reproduced with permission. Copyright 2021 Wiley-VCH.

Table 1. Summary of Various Sulfide-Based SEs and Their Properties

class/type		crystallinity	composition	ionic conductivity (S cm ⁻¹)	shear modulus (GPa) ⁴⁵	ref
glass glass-ceramic crystalline	argyrodite thio-LISICON	amorphous partially crystalline crystalline	$x \text{Li}_2 \text{S} - (100 - x) \text{P}_2 \text{S}_5$ $x \text{Li}_2 \text{S} - (100 - x) \text{P}_2 \text{S}_5$ $\text{Li}_6 \text{PS}_3 \text{X} \ (\text{X} = \text{Cl}, \text{Br}, \text{I} \cdots)$ $\text{Li}_x M_{1-y} M'_y \text{S}_4 \ (\text{M} = \text{Si}, \text{Ge}, \text{Sn}, \text{Zr} \ M' = \text{P}, \text{Al}, \text{Zn}, \text{Ga}, \text{Sb})$	$10^{-3} - 10^{-4}$ 10^{-3} $10^{-2} - 10^{-3}$ 10^{-3}	5-10 5-10 0 10-15	46 47 48 49–51
	LGPS-type		$\operatorname{Li}_{x} \operatorname{M}_{y} \operatorname{P}_{2} S_{12} \ (M = \operatorname{Si}, \operatorname{Ge}, \operatorname{Sn})$	10^{-2}	10-15	44,52,53

and suppress crack propagation caused by the volume changes of active materials, and maintain enough elasticity to withstand roll-to-roll processing and calendering stresses. These mechanical requirements should not compromise ionic transport, so the membrane exhibits high bulk ion conductivity and low charge transfer resistance at both the cathode/ electrolyte and anode/electrolyte interfaces. The Above all, the SE membrane must be made as thin as possible while still offering robust mechanical integrity and reliable electrochemical performances to maximize the overall energy density of the battery. Both gravimetric and volumetric energy densities are predicted to rise sharply as the thickness of the SE membrane decreases (Figure 1c). In particular, reducing the SE membrane to below 30 μ m is considered essential for achieving an energy density higher than 400 Wh kg⁻¹.

Among the various SEs under investigation, sulfide-based SEs stand out as one of the most promising candidates due to their high room-temperature ionic conductivities (up to 10⁻² S cm⁻¹) and inherent mechanical softness, which eliminates the need for high-temperature sintering. This review focuses on the fabrication of sulfide-based SE membranes for application in ASSBs. We first outline the primary challenges associated with SE membrane development, including

minimizing membrane thickness, achieving high ionic conductivity while blocking electronic leakage, ensuring mechanical robustness, and enabling scalable manufacturing. We then introduce state-of-the-art membrane fabrication techniques such as solution casting, scaffold-assisted film formation, dry film processing via binder fibrillation or thermocompression, and compaction methods such as warm isostatic pressing (WIP), along with key characterization approaches for evaluating membrane quality and performance. Finally, we propose future research directions aimed at facilitating the integration of ultrathin sulfide-based SE membranes into commercially viable ASSB systems.

2. OVERVIEW OF SULFIDE SES

2.1. Classification of Sulfide SEs. Sulfide SEs are well-known for their superionic lithium conductivities at room temperature and low activation energies, primarily due to the presence of highly polarizable anions. Based on their structural characteristics, sulfide SEs are broadly classified into three categories based on their structure: glass, glass—ceramic, and crystalline electrolytes (Table 1).

Glass electrolytes are fully amorphous materials that lack long-range structural order. They are typically composed of

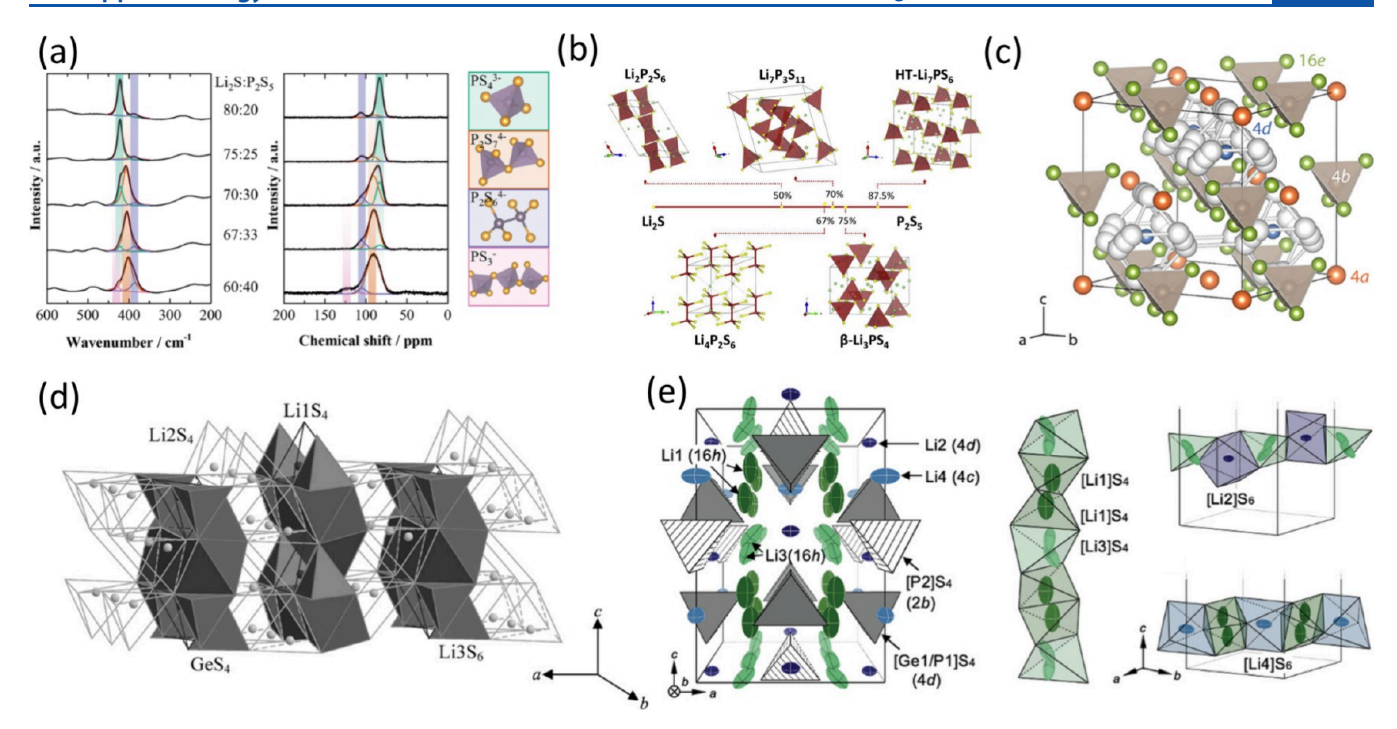


Figure 2. (a) Raman and ³¹P MAS NMR spectra of Li₃PS₄ (LPS) glass electrolytes with different (Li₂S)_x-(P₂S₅)_{100-x} stoichiometries based on various thiophosphate building units. Reproduced with permission. ²⁸ Copyright 2017 Royal Society of Chemistry. (b) Crystal structures of representative glass-ceramic electrolytes in the Li₂S-P₂S₅ binary system at various ratios. Reproduced with permission. ³³ Copyright 2018 Elsevier. (c) Crystal structure of argyrodite-type Li₆PS₅X. Reproduced with permission. ³⁶ Copyright 2019 American Chemical Society. (d) Schematic of crystalline structure of a representative thio-LISICON, Li₄GeS₄. Reproduced with permission. ³⁸ Copyright 2002 Elsevier. (e) Crystal structure of Li₁₀GeP₂S₁₂ (LGPS). Reproduced with permission. ³⁹ Copyright 2020 Wiley-VCH.

 Li_2S and various metal sulfides $(M_x\text{S}_v, \text{ where } M = \text{B, Al, Si, P,}$ Ge, Sn, Sb, with y chosen for charge balance) in different molar ratios. Compared with their crystalline counterparts, glass electrolytes often exhibit higher ionic conductivity due to their isotropic networks, open structure, and large free volume.²⁷ Among these, the binary $xLi_2S-(100-x)P_2S_5$ system has been the most extensively studied. In this composition, Li₂S acts as a network modifier, while P₂S₅ serves as a network former, producing a range of thiophosphate units such as orthothiophosphate (PS_4^{3-}) , pyro-thiophosphate $(P_2S_7^{4-})$, metathiodiphosphate $(P_2S_6^{2-})$, and hypo-thiodiphosphate $(P_2S_6^{4-})$ (Figure 2a).²⁸ When the Li₂S content lies within the range of 60-80 mol%, increasing Li₂S shifts the structural motif from bridging P₂S₇⁴⁻ units to isolated PS₄³⁻ tetrahedra. At an optimal 75:25 Li₂S:P₂S₅ ratio, where PS₄³⁻ units dominate, the material exhibits the highest ionic conductivity and lowest activation energy.²⁹

Glass-ceramic electrolytes are produced by the partial crystallization of sulfide glasses through thermal annealing, producing SEs that contain both amorphous and crystalline phases. These electrolytes combine the mechanical flexibility of the glassy matrix with the superior ionic conductivity of the embedded crystalline domains. Prominent examples include $\rm Li_7P_3S_{11}$ (derived from $70\rm Li_2S-30P_2S_5)$, 30 β - $\rm Li_3PS_4$ (from $75\rm Li_2S-25P_2S_5)$, 31 and $\rm HT$ - $\rm Li_7PS_6$ (from $87.5\rm Li_2S-12.5P_2S_5)^{32}$ (Figure 2b). 33 The ionic conductivity of glass-ceramics is largely governed by the relative fractions of glassy and crystalline phases, which depend on the annealing temperature and ball milling conditions. Among them, $\rm Li_7P_3S_{11}$ has garnered significant attention due to its high ionic conductivity of 1.58×10^{-3} S cm $^{-1}$ at room temperature. 34

Crystalline electrolytes have attracted intense interest for their outstanding ionic conductivities, which are comparable to those of conventional liquid electrolytes. Popular crystal structures include argyrodite-type (Li₆PS₅X, X = Cl, Br, or I), 35,36 thio-LISICON-type (Li_x $M_{1-y}M'_yS_4$, M = Si, Ge, Sn, Zr; M'= P, Al, Zn, Ga, Sb), 37 and LGPS-type (Li₁₀GeP₂S₁₂) compounds (Figure 2c-e). 36,38,39 The argyrodite structure was first identified in 1885 from the mineral Ag₈GeS₆, which exhibited remarkably high Ag⁺ mobility, 40 and was later adapted to the lithium analogue (Li₆PS₅X) by Deiseroth et al.35 Subsequent development led to a broader family of lithium argyrodites with the general formulas Li₇MS₆ or Li_6MS_5X (M = P, As, and X = Cl, Br, I),³⁵ among which Li₆PS₅Cl and Li₆PS₅Br exhibit high room-temperature ionic conductivities in the range of 10^{-2} to 10^{-3} S cm⁻¹. Recently, various families of argyrodite have been vigorously studied to increase ionic conductivity, such as Li-deficient structure, 41 BH₄⁻ substituted argyrodite, ⁴² and Cl–Br codoped structure, ⁴³ showing superior ionic conductivity beyond 10 mS cm⁻¹. Thio-LISICONs, derived from the oxide-type LISICON conductors by substituting oxygen with sulfur, benefit from the enhanced polarizability of the sulfide anions, resulting in improved Li+ mobility. Kamaya et al. reported the LGPS phase, 44 which demonstrates an exceptionally high Li+ conductivity of $1.2 \times 10^{-2} \text{ S cm}^{-1}$ at room temperature. Its crystal structure is composed of (Ge_{0.5}P_{0.5})S₄, PS₄, LiS₄ tetrahedra, along with LiS₆ octahedra, forming one-dimensional Li⁺ diffusion pathways along the c-axis (Figure 2e).³⁹ The discovery of these highly conductive crystalline sulfides with Li⁺ conductivities above 10⁻² S cm⁻¹—has established sulfide SEs as one of the most promising replacements for liquid electrolytes in next-generation ASSBs.

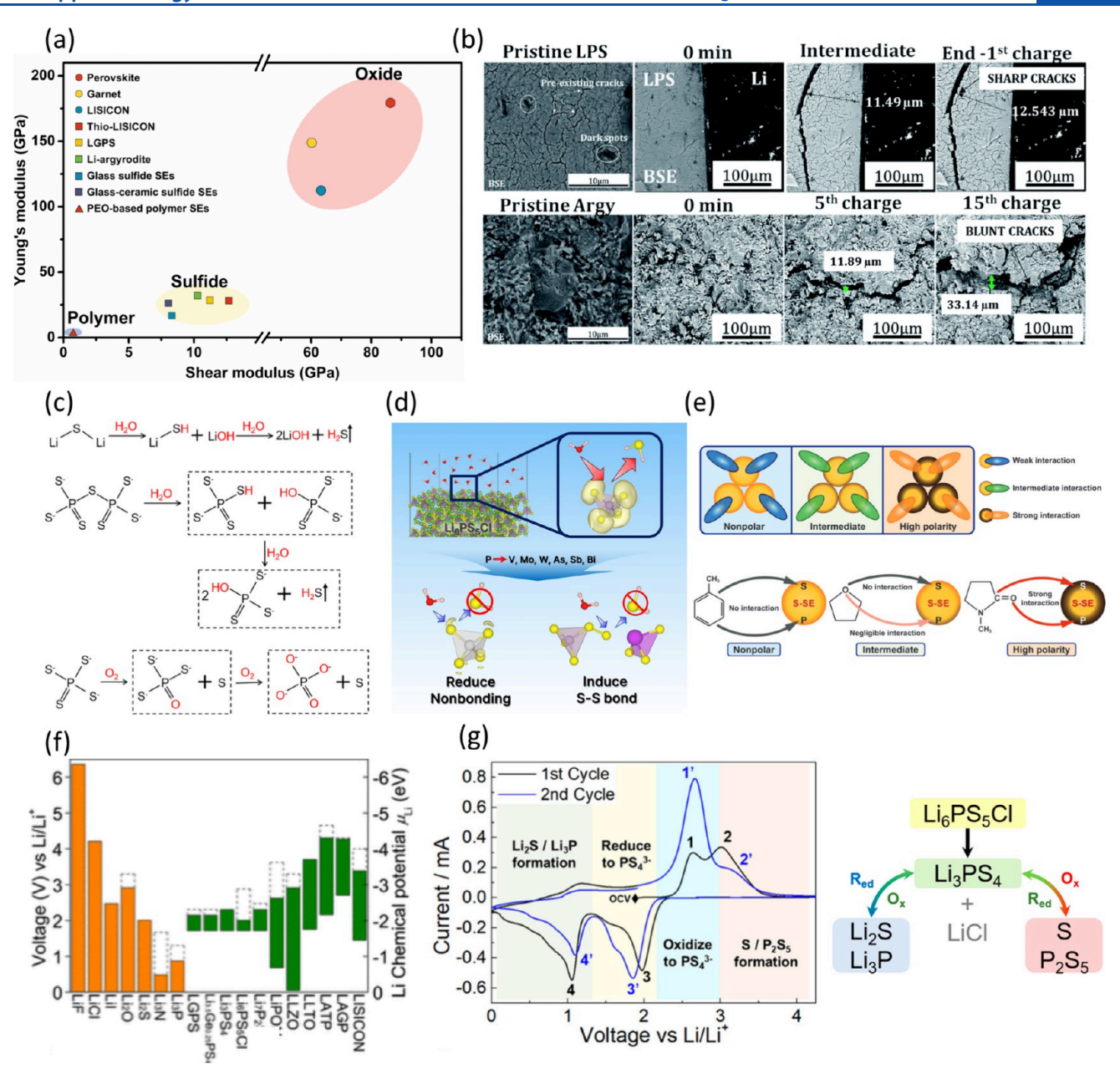


Figure 3. (a) Ashby plot showing the shear modulus and Young's modulus for different types of SEs. Reproduced with permission. ⁴⁵ Copyright 2023 Royal Society of Chemistry. (b) Backscattered electron (BSE) images showing the evolution of solid electrolytes during cycling for β-Li₃PS₄ and Li₆PS₅Cl, highlighting the formation and propagation of cracks. Reproduced with permission. ⁵⁵ Copyright 2022 Royal Society of Chemistry. (c) Decomposition reactions of sulfide SEs in humid air showing hydrolysis of Li₂S, P₂S₇. Reproduced with permission. ⁵⁶ Copyright 2023 AAAs. (d) Schematic of the degradation mechanism of Li₆PS₅Cl electrolyte in humid air and doping strategies to enhance moisture stability. Reproduced with permission. ⁵⁹ Copyright 2016 Elsevier. (e) Schematic diagrams illustrating the polarity-dependent solvent compatibility of sulfide solid electrolytes and potential nucleophilic attacks by solvents. Reproduced with permission. ⁶² Copyright 2022 Royal Society of Chemistry. (f) Electrochemical window of various solid electrolytes and binary lithium compounds. Reproduced with permission. ⁶³ Copyright 2015 American Chemical Society. (g) Cyclic voltammograms of Li–In | Li₆PS₅Cl | Li₆PS₅Cl-C half cells, and suggested electrochemical reactions occurring in Li₆PS₅Cl electrolyte. Reproduced with permission. ⁶⁴ Copyright 2019 American Chemical Society.

2.2. Characteristics of Sulfide SEs. In addition to their high ionic conductivity, sulfide SEs offer favorable mechanical properties. With Young's moduli ranging from 10 to 30 GPa—considerably lower than those of oxide SEs—sulfides exhibit inherently ductile behavior (Figure 3a). 45,54 Their mechanical softness allows powders to be cold-pressed into dense membranes without the need for high-temperature sintering, thereby promoting intimate interfacial contact between the electrolyte and electrodes and simplifying the overall fabrication process. Moreover, their elastic nature accommo-

dates stresses from volume changes of the electrode during charge/discharge cycles, contributing to sustained interfacial integrity. However, the low modulus of sulfide SEs also raises concerns for lithium dendrite penetration and crack propagation induced by electro-chemo-mechanical stress, particularly when sulfides are used as separating membranes (Figure 3b). To address these issues, it is important to develop mechanically robust SE layers reinforced with suitable binders or scaffolds that can provide sufficient strength while preserving electrochemical performance.

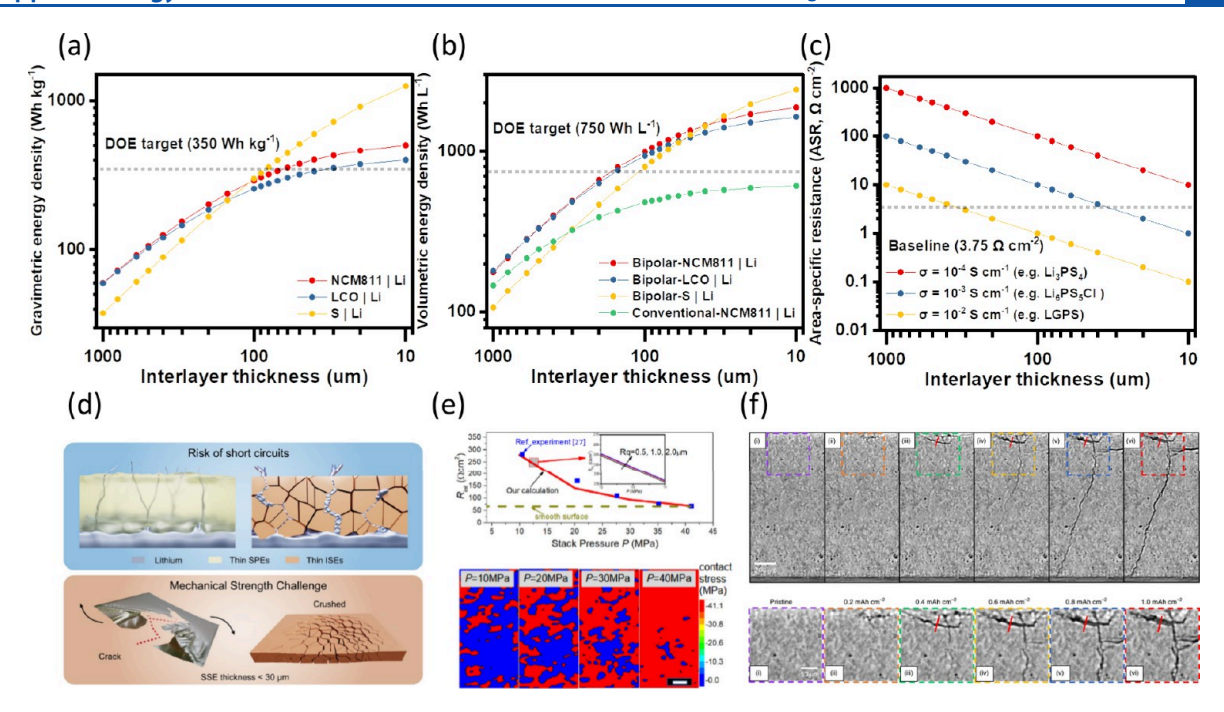


Figure 4. (a) Estimated gravimetric and (b) volumetric energy densities for various cell configurations as a function of SE thickness, calculated based on the "SolidPAC" model. (c) Area-specific resistance as a function of SE thickness across a range of SE conductivities. Reproduced with permission. Copyright 2022 Cell Press. (d) Key challenges in reducing the solid-state electrolyte thickness. Reproduced with permission. Copyright 2024 Elsevier. (e) Interfacial resistance–pressure relationship and Li surface stress maps under varying stack pressures. Reproduced with permission. Copyright 2020 Cell Press. (f) In situ phase-contrast XCT virtual cross sections during a single plating of a LilLi₆PS₃CllLi cell. Reproduced with permission. Copyright 2021 Nature Publishing Group.

Sulfide SEs also suffer from severe chemical instability issues. In ambient air, they hydrolyze even in the presence of trace moisture, releasing toxic H2S gas and thereby complicating handling and processing (Figure 3c). 56 The irreversible sulfur loss that occurs during hydrolysis leads to permanent structural degradation of sulfides.⁵⁷ This vulnerability can be rationalized using the hard-soft-acid-base (HSAB) theory. According to this principle, small hard acid ions—such as P5+ in thiophophate (PS_4^{3-}) units—tend to form stronger bonds with hard base ions like O^{2-} (from H_2O), while larger and more polarizable soft acids (e.g., Sn^{4+} , As^{5+}) preferentially bind to soft base ions such as S^{2-58} Upon exposure to water, the hard acid P⁵⁺ in PS₄³⁻ interacts with O²⁻, leading to cleavage of the P-S bonds and degradation of the electrolyte structure. One strategy to improve moisture stability involves substituting P5+ with softer cations such as As5+ or Sb5+, which enhances the P-S bond strength and reduces reactivity with water (Figure 3d).⁵⁹ Other approaches include partial oxygen substitution (i.e., replacing a portion of S^{2-} with O^{2-}), and incorporating metal oxide nanoparticles such as ZnO or Bi₂O₃, which can capture released H2S gas and mitigate degradation. 7,60,61 Sulfide SEs are also highly sensitive to many polar solvents. Polar solvents readily react with building units of sulfides, such as PS₄³⁻, P₂S₆⁴⁻, to generate nonionic conducting impurities and induce collapse of their crystal structure (Figure 3e). 62 Therefore, nonpolar or less polar solvents are more suitable for solution processing, as they have only limited interactions with sulfides. In addition, restrictions on solvent selection limit the choice of compatible binders, which will be further discussed in a later section together with the solution casting of SE membranes.

Another critical challenge associated with sulfide SEs is their narrow electrochemical stability window. Thermodynamically,

sulfides are unstable at both the anode and the cathode interfaces. LGPS and Li₆PS₅Cl are predicted to be electrochemically stable only within narrow potential ranges of 1.71-2.14 and 1.7-2.01 V vs Li⁺/Li, respectively (Figure 3f).⁶³ However, in practical applications, battery cells typically operate over a much broader voltage range—from 0 V to nearly 5 V. This apparent discrepancy is kinetically tolerated due to the formation of passivating interphase layers and the intrinsically low electronic conductivity of sulfide SEs.⁶⁰ For example, when Li₆PS₅Cl is in contact with the Li metal, it undergoes decomposition during cycling, producing Li₂P, Li₂S, and LiCl. These products collectively form a stable interphase that suppresses further electrolyte degradation and inhibits lithium dendrite growth (Figure 3g).64 However, in SEs containing semiconducting elements such as Ge or Sb (e.g., LGPS), reductive decomposition can yield Li-metal alloys such as Li₃Sb or Li_xGe. These conductive phases contribute to undesirable electronic leakage across the interface, accelerating parasitic side reactions and increasing interfacial resistance. Therefore, the design of sulfide SE membranes must carefully consider the interfacial compatibility with lithium metal. In many cases, surface protection strategies—such as applying chemically stable interfacial coatings—are necessary to enhance interfacial stability and suppress detrimental side reactions at the electrode-SE electrolyte interface.

3. CHALLENGES IN SULFIDE-BASED SE MEMBRANES

The SE membrane—an essential component unique to ASSBs and absent in conventional LIBs—must be carefully engineered to enable the practical realization of ASSB technology. To achieve high-energy-density ASSBs, the SE membrane must be made sufficiently thin while still fulfilling several critical functions: (1) serving as an electronic insulator

to prevent short-circuiting between the anode and cathode, (2) providing fast and uniform lithium-ion transport, and (3) offering mechanical robustness to ensure long-term structural stability during battery operation. In addition to these performance requirements, process scalability and technoeconomic feasibility are also key considerations for translating ASSB technology into practical applications. Due to their extreme sensitivity to moisture, scaling up the production of an ultrathin sulfide SE membrane presents significant challenges. The entire manufacturing process must be conducted under strict environmental controls, such as ultralow dew point dry rooms or inert atmosphere glove boxes, and supported by specialized safety infrastructure to manage H₂S emissions. In this section, we discuss the major challenges in realizing ultrathin sulfide-based SE membranes with a focus on thickness reduction and mechanical integrity for scalable manufacturing.

3.1. Thickness Considerations. The thickness of the SE membrane plays a pivotal role in determining the overall energy density of the ASSBs. Despite ongoing advancements, many laboratory-scale studies continue to rely on pelletized sulfide SE membranes with thicknesses of approximately 800 μ m and areas of around 1.5 cm² to investigate cell chemistries. However, such thick pellets are impractical for high-energydensity applications and lead to elevated processing costs due to their complex fabrication. Therefore, the transition from bulky pellet configurations to ultrathin, sheet-type SE membranes is essential for the development of commercially viable ASSBs. Modeling studies using the SolidPAC toolkit have quantitatively evaluated the impact of SE membrane thickness on cell-level gravimetric energy density (Figure 4a and Table S1).²⁰ For instance, to meet the U.S. Department of Energy (DOE) target of 350 Wh kg $^{-1}$, the Li₆PS₅Cl SE membrane must be reduced to below 60 µm in NCM811|Li cells, 29 μ m in LiCoO₂|Li cells, and 80 μ m in S|Li cells. Similar projections across various cell chemistries suggest that achieving such energy targets generally requires SE thicknesses in the range of 20–80 μ m. Thinner SE layers also contribute to the improved volumetric energy density. For example, reaching the DOE's volumetric energy target of 750 Wh L⁻¹ would likely require SE membranes thinner than 200 μ m, especially when combined with bipolar cell designs that minimize inactive volume compared to conventional monopolar stacking (Figure 4b and Table S1). Sensitivity analyses further identify SE membrane thickness as one of the most influential factors affecting energy density, often surpassing the impact of parameters such as the N/P ratio or catholyte fraction.²⁰

In addition to the energy density, the SE thickness also critically affects the internal resistance of the cell. The internal resistance of the cell can be expressed by the area-specific resistance (ASR), defined as

$$ASR = R \times A = L/\sigma$$

where R is resistance, A is electrode area, L is SE membrane thickness, and σ is ionic conductivity of SE.

For comparison, a typical liquid electrolyte with an ionic conductivity of approximately 20 mS cm $^{-1}$ in a 25 μ m-thick separator yields an ASR of 0.125 Ω cm 2 , which increases to 3.75 Ω cm 2 when accounting for the tortuosity of the porous separator. To achieve a comparable ASR using Li₆PS $_5$ Cl (with an ionic conductivity of 10^{-3} S cm $^{-1}$), the SE membrane must be thinned to approximately 40 μ m (Figure 4c). In contrast, LPS-based electrolytes cannot attain a similar ASR

even when reduced to 10 μ m thickness, indicating the importance of both thickness and intrinsic ionic conductivity of the SE membrane. Reducing the thickness of the SE membrane not only boosts gravimetric and volumetric energy density but also plays a key role in minimizing internal resistance. In practice, SE membrane thicknesses below 30 μ m are typically required for ASSBs to achieve competitive energy and power performance.

3.2. Mechanical Stability. Producing a uniform, defectfree SE membrane with a thickness of only several tens of micrometers—while preserving mechanical stability throughout processing and cell operation—remains a major challenge. Although the sulfide SEs are mechanically softer than their oxide-based counterparts, they are still inherently brittle. The cold-pressed sulfide pellets, in particular, are prone to cracking and fracturing. 18 Mechanical failure of the SE membrane can result in (1) internal short circuits caused by lithium dendrite penetration and (2) structural degradation during cycling (Figure 4d).66 According to the Monroe-Newman model, when the shear modulus of SE exceeds at least twice that of Li (3.4 GPa), dendrite growth can be suppressed. ¹⁴ Although sulfide SEs possess shear moduli in the range of 6-11 GPa, sulfide-based ASSBs still suffer from mechanical failure.70 Mitigating Li dendrite growth and crack propagation depends not only on the intrinsic mechanical properties of solid electrolytes but also on the mechanical strength of SE membranes and the quality of interfacial contact with electrodes. Ultrathin, freestanding membranes fabricated solely by pressing the sulfide SE powder are especially susceptible to crumbling under minimal mechanical stress, and this fragility becomes even more pronounced as the SE membrane thickness decreases. The issue is further exacerbated when scaling up to the large-area sheet-type membranes as thin films with large lateral dimensions are more vulnerable to stress accumulation, defect formation, and mechanical damage during roll-to-roll processing, drying, and handling.

To enhance the mechanical strength, polymeric binders or scaffold supports are commonly employed as mechanical reinforcements. Even small additions of binder—typically 0.5—10 wt% relative to the total SC—can significantly enhance the toughness and flexibility of the membrane. Since even minor defects or microcracks can serve as initiation sites for crack propagation, strict quality control during membrane fabrication is crucial. Inline inspection techniques, along with postprocessing methods such as mild thermal annealing, calendering, and pressurization, can help minimize surface flaws and internal voids, thereby improving mechanical reliability.

Furthermore, the SE membrane must maintain stable interfacial contact with the electrodes under low stack pressures, typically below 2 MPa. Under such ultralow-pressure conditions, nonuniform stress distribution and particle-to-particle contact within the SE layer can lead to increased internal resistance and potential delamination at the electrode—electrolyte interfaces (Figure 4e).⁶⁷ Critically, interfacial voids have been identified as preferential pathways for lithium dendrite growth. In situ X-ray computed tomography (XCT) studies have directly visualized lithium dendrite propagation along pre-existing interfacial gaps or microcracks in sulfide SEs (Figure 4f).⁶⁸ Without sufficient fracture toughness and fatigue resistance, repeated mechanical stresses during cycling can accelerate crack formation and ultimately result in catastrophic cell failure.

The mechanical and interfacial challenges discussed above highlight the critical role of fabrication strategies in determining the performance and reliability of SE membranes for practical application. Accordingly, the following section introduces various fabrication approaches for sulfide SE membranes, outlining their respective principles, advantages, and limitations.

4. FABRICATION METHODS FOR SULFIDE SE MEMBRANES

4.1. Preparation of SE Membrane: Free-Standing vs Double Casting. Generally, the SE membrane is fabricated by one of two primary approaches: free-standing membrane formation or direct double casting onto a preformed electrode laminate (Figure 5).⁷

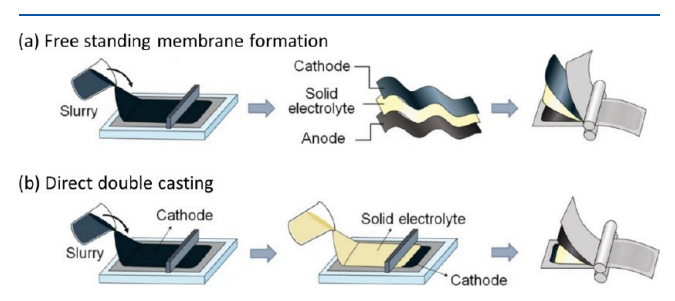


Figure 5. Schematic of two solid electrolyte membrane fabrication approaches: (a) free-standing membrane formation and (b) direct double casting onto a preformed electrode laminate. Reproduced with permission. Copyright 2021 American Chemical Society.

In the free-standing film approach, a self-supporting electrolyte membrane is produced independently of the electrodes, either by solution casting on a sacrificial substrate followed by peel-off, scaffold-assisted infiltration, or dry film processing. Once fabricated, the resulting SE membrane is sandwiched between the cathode and anode and compressed together for cell assembly. This strategy enables independent and precise control over the membrane thickness and mechanical properties. Decoupling electrolyte fabrication from electrode preparation enhances compatibility with diverse electrode chemistries and allows for separate optimization of electrode and electrolyte materials. However, producing ultrathin membranes with sufficient mechanical integrity remains a challenging. Moreover, surface defects, such as roughness and pinholes, must be minimized to mitigate the formation of interfacial voids at the electrodes–electrolyte interface that can occur during layer stacking. ⁷²

In contrast, the double-casting approach involves directly coating an SE slurry onto a preformed electrode laminate. This method can be applied to both composite cathodes and anodes. 73,74 However, casting slurries directly onto Li metal foils is generally avoided, because Li is highly reactive with sulfide SEs and many solvents. The double-casting method forms a conformal and integrated electrode—electrolyte interface, substantially reducing interfacial resistance. Additionally, the pre-existing electrode layer provides mechanical support, allowing fabrication of ultrathin SE layers. However, since double casting generally relies on solution processing, it requires careful selection of solvent—binder systems and meticulous control over slurry formulation, coating conditions, and drying parameters. Inadequate control can lead to chemical degradation, phase

intermixing, or side reactions that may impair the electrode performance or compromise interfacial adhesion.

In the following section, various fabrication techniques for SE membranes, including wet and dry processing, are discussed (Table 2). While thin-film deposition techniques such as physical vapor deposition (PVD), atomic layer deposition (ALD), and spray coating are also widely used to produce submicrometer SE layers for thin-film or model cells, these approaches are costly and unsuitable for fabricating large-format membranes. Accordingly, this review focuses on fabrication methods that are scalable for the development of practical bulk-type ASSBs.

4.2. Solution Casting. Solution casting is a method for preparing SE layers by first dispersing SE particles and polymeric binders in solvents to form a uniform slurry, then coating the slurry onto a substrate using techniques such as slot-die coating, doctor-blading, or tape casting, and subsequently drying it to yield a robust thin film. This approach not only enables continuous, large-area processing but also benefits from existing solution processing infrastructure developed for liquid-based LIB manufacturing. To advance the scalability of this method, the development of tailored solvent-binder pairs along with optimized casting, drying, and post-treatment techniques is critical. In solution processing, film quality strongly depends on parameters such as coating thickness, slurry viscosity, and the adhesion properties of the binder. Using this method, SE membranes with thicknesses ranging from 25 to 75 μ m have been reported. ^{11,78}

4.2.1. Key Slurry Parameters: Solid Content and Binder Content. Solid content (SC), the mass fraction of SE and binder in the slurry, critically affects the slurry viscosity and coatability, volumetric shrinkage during drying, and thickness and uniformity of the as-cast layer. Higher SC increases the slurry viscosity and causes particle aggregation. At very high SC, the slurry becomes overly viscous for reliable film thickness control, and rapid solvent evaporation can induce binder migration and uneven particle distribution, resulting in surface defects and disrupted conduction pathways. By contrast, excessively low SC promotes the formation of pinholes and cracks in the dried film. Therefore, SC is typically regulated between 50 and 60 wt%. As shown in Figure 6a, increasing SC and BC increases the slurry viscosity across the whole shear-rate range. This relationship is crucial, as viscosity directly affects coatability of the slurry and the presence of casting defects.

Binder content (BC), the mass fraction of binder relative to the total solid component sum of SE and binder, is commonly set between 1 and 3 wt% to ensure the formation of stable, thin film SE layers. ⁷⁸ While incorporating binder enhances the mechanical strength of the film, it also reduces ionic conductivity, because most binders are nonionic polymers that block ion transport between electrolyte particles. The critical BC at which ionic conductivity begins to decline varies depending on the chemical structure and the ionic resistivity of the binder. For instance, when poly(isobutylene) (PIB) was used, the SE layer retained relatively high ionic conductivity at BC below 2 wt %. However, once BC exceeded 5 wt%, interfacial resistance increased sharply, and overall ionic conductivity dropped. ⁷⁸

4.2.2. Solvent Compatibility and Dispersion Stability. Due to their chemical instability toward polar solvents, solution casting processes of sulfide SEs are limited to nonpolar or low-polarity solvents. For instance, N-methyl-2-pyrrolidone (NMP), a highly polar solvent commonly used in LIB electrode fabrication, reacts vigorously with sulfide SEs, disrupting their crystal structures and drastically decreasing their ionic conductivity by several orders of

Table 2. Comparative Summary of Fabrication Routes for Sulfide-Based SE Membranes

route	scalability/cost	achievable minimum thickness	interfacial quality	mechanical robustness	materials compatibility
solution casting	good	good	good	fair	fair
scaffold	fair	poor	fair	excellent	good
dry film—PTFE fibrillation	good	fair	good	good	excellent
dry film—thermocompression	fair	fair	good	fair	good

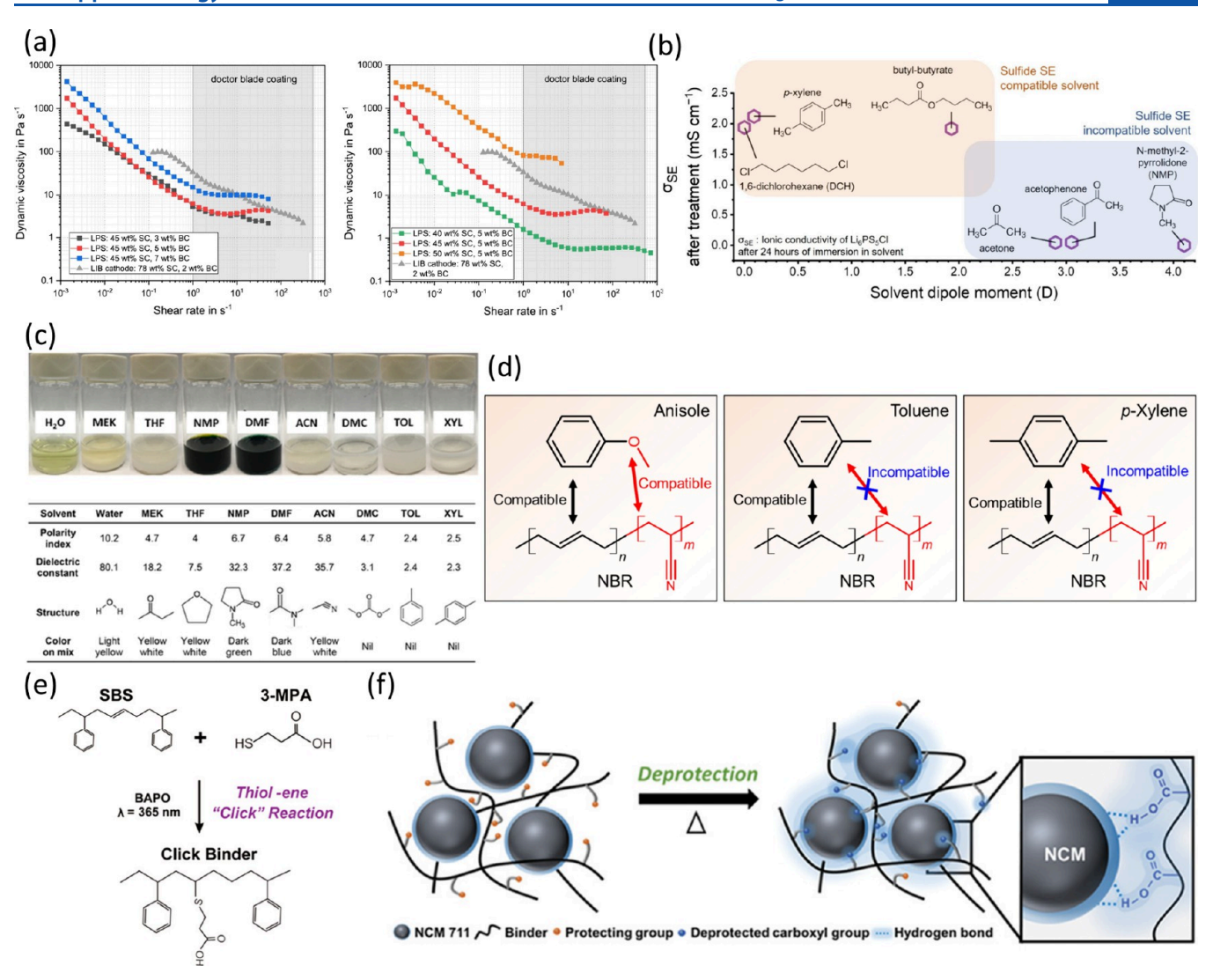


Figure 6. (a) Effect of the solid content (SC) and binder content (BC) of the LPS/HNBR slurry on the viscosity change according to the shear rate. Reproduced with permission. Copyright 2023 Elsevier (b) Net dipole moments of various solvents, including typical low-polarity solvents used for solution-processing of sulfide-based ASSBs, and the ionic conductivity of LPSCl after solvent treatment (24 h of immersion followed by drying). Reproduced with permission. Copyright 2025 American Chemical Society. (c) Color change of common solvents used in battery electrode processing after the addition of Li₂P₃S₁₁ and their key properties. Reproduced with permission. Deprised 2019 American Chemical Society. (d) Molecular compatibility between each unit of NBR copolymer and solvents (anisole, toluene, and *p*-xylene). Reproduced with permission. Copyright 2025 Elsevier. (e) Synthesis of the click binder using the click (thiol—ene) reaction between SBS and mercaptocarboxylic acid. Reproduced with permission. Copyright 2018 American Chemical Society. (f) Schematic illustration of the protection—deprotection chemistry for the adhesive interaction between the polymeric binder and active material in the composite cathode. Reproduced with permission. Copyright 2020 Wiley-VCH.

magnitude. In contrast, exposure to low-polarity solvents such as pxylene preserves the ionic conductivity of sulfides (Figure 6b).⁷⁴ As a result, nonpolar solvents such as toluene, xylene, and anisole are generally used in the solution processing of sulfide SEs.⁸³ When sulfide SEs are dispersed in nonpolar or less polar solvents, the suspensions retain the original gray-white color of SEs, becoming only slightly cloudy. By contrast, polar solvents such as NMP and water yield dark black or clear yellow solutions, indicating substantial chemical reactions (Figure 6c).⁷⁹ More recently, various organic ester solvents, such as butyl butyrate and hexyl butyrate, have gained popularity. They uniformly disperse sulfide SEs without agglomeration and preserve high ionic conductivity after drying.⁸⁴ Although esters contain polar functional groups, some of them can still be compatible with sulfides when their alkyl chains are sufficiently long or their molecular weight is high enough to reduce the overall polarity. In contrast, strongly polar solvents such as alcohols or carboxylic acids remain incompatible even when modified with

extended alkyl chains. Furthermore, increasing the molecular weight to suppress polarity often leads to excessive viscosity, making such solvents impractical for slurry casting.

An ideal solvent must disperse SE powders homogeneously, possess adequate viscosity that prevents sedimentation, have appropriate vapor pressure to avoid rapid evaporation and binder migration, and dissolve the polymeric binder effectively. Thus, identifying a solvent with suitable polarity and rheological properties is a top priority in the slurry formulation of sulfide SEs.

4.2.3. Binder Selection Strategies. Binders control slurry rheology and play an important role in securing the physical adhesion and mechanical flexibility of the film. However, the solvent restrictions imposed by sulfides limit binder selection. Following the "like dissolves like" principle, nonpolar or low-polarity solvents can only dissolve polymers with similarly low polarity. As a result, rubber-based polymers such as polybutadiene (PB), ⁸⁵ polystyrene-polybutadiene rubber (SBR), ⁸⁶ polyacrylonitrile-polybutadiene rubber (NBR)⁸⁷ are

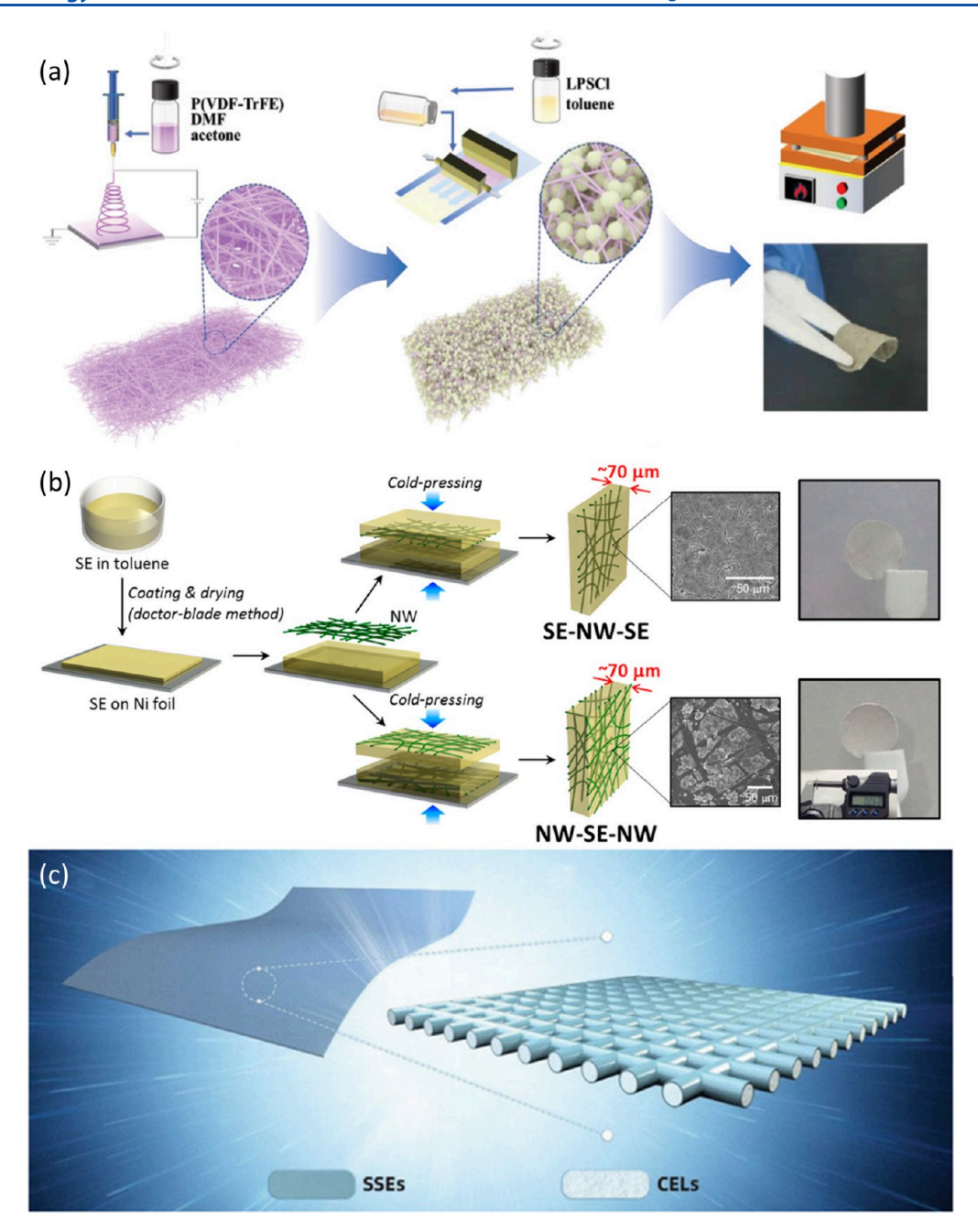


Figure 7. (a) Schematic illustration of the fabrication procedure of the interpenetrating LPSCl@P(VDF-TrFE) CSEs via an electrospinning-infiltration-hot-pressing method. Reproduced with permission. Copyright 2022 Wiley-VCH. (b) Schematic illustration of nonwoven (NW) scaffold SE films with two different structures (SE–NW–SE and NW–SE–NW). Reproduced with permission. Copyright 2015 American Chemical Society. (c) Schematic illustrations of the free-standing and flexible SSE film and the intercrossed CELs skeleton coated with a thin sulfide SSE layer to construct a 3D interconnecting ionic-conducting framework. SSEs represent the sulfide solid-state electrolytes, and CELs represent the cellulose skeleton. Reproduced with permission. Copyright 2021 Wiley-VCH.

commonly used. However, the low polarity of these binders poses challenges. The adhesive strength of polymeric binders typically arises from polar—polar interactions between the binder and electrode components (Figure 6e). ^{74,80} Polymers with low polarity tend to exhibit weak adhesion, which undermines the primary function of the binders. To address this, various strategies have been explored to introduce polar functional groups into the nonpolar polymer backbone, thereby improving the mechanical strength and interfacial adhesion. These include grafting carboxylic acid groups through click reaction (Figure 6e), ⁸¹ thermally induced post-deprotection after casting to reveal poly(acrylic acid) (Figure 6f), ¹⁰ or the use of block copolymers containing polar blocks such as acrylates. ⁸⁸ In addition to synthetic rubber-based binders, the semisynthetic polymer type ethyl

cellulose is also broadly used with sulfide SEs, serving as both a dispersing agent and a moderately polar binder. 89

Because most binders are ionically insulating, excessive BC hinders ion transport and lowers the ionic conductivity of the SE membrane. Therefore, careful optimization of the binder chemistry, composition, and content is essential. To overcome this, Li⁺-conducting binders including Polyethylene glycol (PEG), polystyrene-PEG (PS-PEG), and NBR incorporated with LiTFSI have been developed.⁸⁸ These ionic conductive binders promote ion transport by forming ionic pathways between SE particles and reducing interfacial resistance.^{90,91} For instance, NBR incorporating Li(G3)TFSI ionic liquid binder has shown improved battery performance by enhancing Li⁺ transport across interfaces.⁹² However, because many Li⁺ ion-conductive

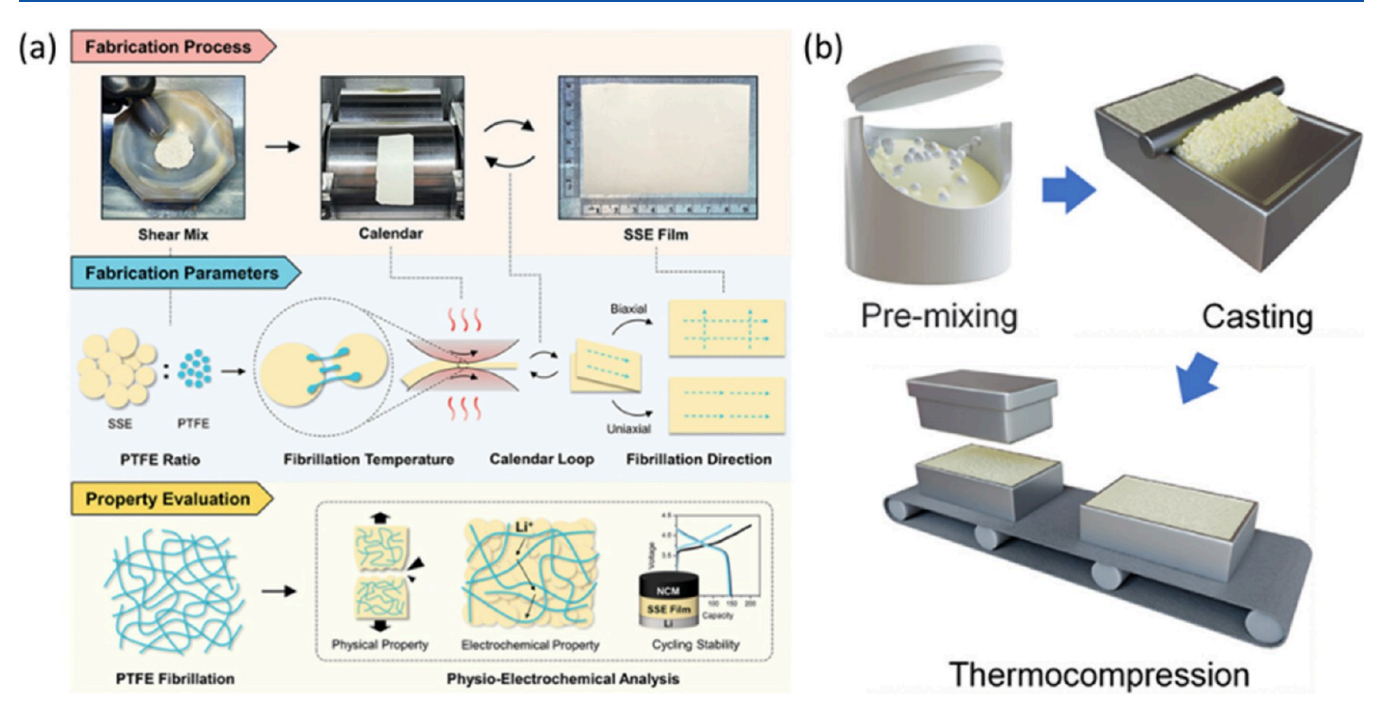


Figure 8. (a) Schematic of an SE membrane made by dry film processing using PTFE as a binder. Reproduced with permission. ¹⁰² Copyright 2023 Wiley-VCH. (b) Schematic of the thermocompression process for dry-film fabrication. Reproduced with permission. ¹⁰⁴ Copyright 2024 Wiley-VCH.

binders include ionic liquids or trace amounts of liquid electrolyte content, careful control of the slurry rheology, compatibility with sulfides, and preservation of the electrode microstructure is required to avoid compromising mechanical or interfacial stability. In some approaches, the binders are removed after thin film formation through heat treatment or solvent washing to eliminate insulating components. For the long-term effects of binder removal remain underexplored. Evaluation in pouch-cell configurations under minimal external pressure is necessary to assess its impact on cycling performance. Overall, the selection of a suitable binder requires systematic consideration of its chemical structure, solubility, electrochemical stability, mechanical properties, and ionic resistance.

4.3. Scaffold Support. Scaffold-assisted infiltration involves impregnating a porous support with an SE slurry, followed by drying to produce a composite membrane reinforced by the scaffold. The incorporation of SE powders into scaffold structures has been extensively investigated since the early stages of ASSB development. A scaffold is a three-dimensional framework designed to provide mechanical support and structural integrity to SE membranes. This strategy enables easy fabrication of thin and flexible SE films with high mechanical strength and continuous ion-conduction pathways and mitigates issues such as cracking or short-circuiting. For scaffold-reinforced SE membranes, reported thicknesses range from 30 to 70 μ m. ^{93,94} In practice, they are typically composed of 70–95 wt% of SE and 5–30 wt% of supporting scaffold. ^{93,95}

Scaffolds have been developed using a variety of materials and architectures, including electrospun polymer networks, nonwoven polymer mats, porous polymer frame supports, and cellulose-membrane-based skeletons (Figure 7). Representative examples are poly(vinylidene fluoride-trifluoroethylene) (P(VDF-TrFE)) polymer networks, poly(paraphenylene terephthalamide) (PPTA) nonwoven scaffolds, cellulose membrane skeletons, and porous polyethylene (PE) separators, all of which have demonstrated the ability to produce thin, mechanically robust SE membranes. Each design offers distinct advantages in terms of mechanical flexibility, ionic conductivity, processability, and scalability for practical applications. This scaffold-supported approach is promising for scaling up, as it can be integrated with existing tape-casting infrastructure by substituting the conventional substrates with porous ones to enable the impregnation of the

SE solution. In such processes, nonuniform infiltration of the SE solution or pore formation during solvent evaporation may increase interfacial resistance, ⁹⁷ and side reactions between the scaffold and SE can occur during annealing. ⁹⁸ Therefore, precise control over several key parameters, including fine-tuning of SE viscosity, and optimization of casting/infiltration, drying, and postdensification conditions, is essential. ⁶⁶

4.4. Dry Film Processing. Despite the advantages of solution processing, the tricky selection condition of the solvent for sulfide SEs continues to pose a major obstacle. Recently, dry film processing has emerged as an environmentally friendly, cost-effective, solvent-free fabrication alternative. This method prevents solvent-induced degradation of sulfide SEs, reduces energy consumption by eliminating solvent drying and recovery processes, and supports a safer, more sustainable manufacturing process that is both environmentally and worker-friendly. However, the absence of solvents makes it more difficult to uniformly mix various solid components, a common challenge in dry processing techniques.

4.4.1. Polytetrafluoroethylene Fibrillation. Polytetrafluoroethylene (PTFE) is the most widely used binder employed in dry mixing electrode fabrication. Its molecular structure consists of two fluorine atoms bonded to each carbon atom along a linear C-C backbone, forming a perfluorinated alkane. This unique chemical structure gives PTFE one of the lowest coefficients of friction among polymers. Accordingly, PTFE can undergo fibrillation under shear stress, allowing it to function as a binder without the need for dissolution in solvents. PTFE fiber-based dry film processing offers advantages in lithium-ion diffusion. Unlike many solution-processable binders that extensively coat SE particles, PTFE forms only limited surface coverage. Given that binder is insulating, reduced binder coverage on SE particles enables faster lithium-ion transport. ¹⁰¹

When subjected to strong mechanical mixing or extrusion, PTFE powder stretches into fibrils. The fibrous structures entangle with SE particles during mixing, reinforcing the composite to form a cohesive SE membrane. Once the self-standing SE membrane is formed, it is calendered to achieve the desired thickness (Figure 8a). With an increasing number of calendering cycles, the degree of PTFE fibrillation improves. As a result, the tensile strength of the filling voids and forming a continuous SE membrane increased while ionic

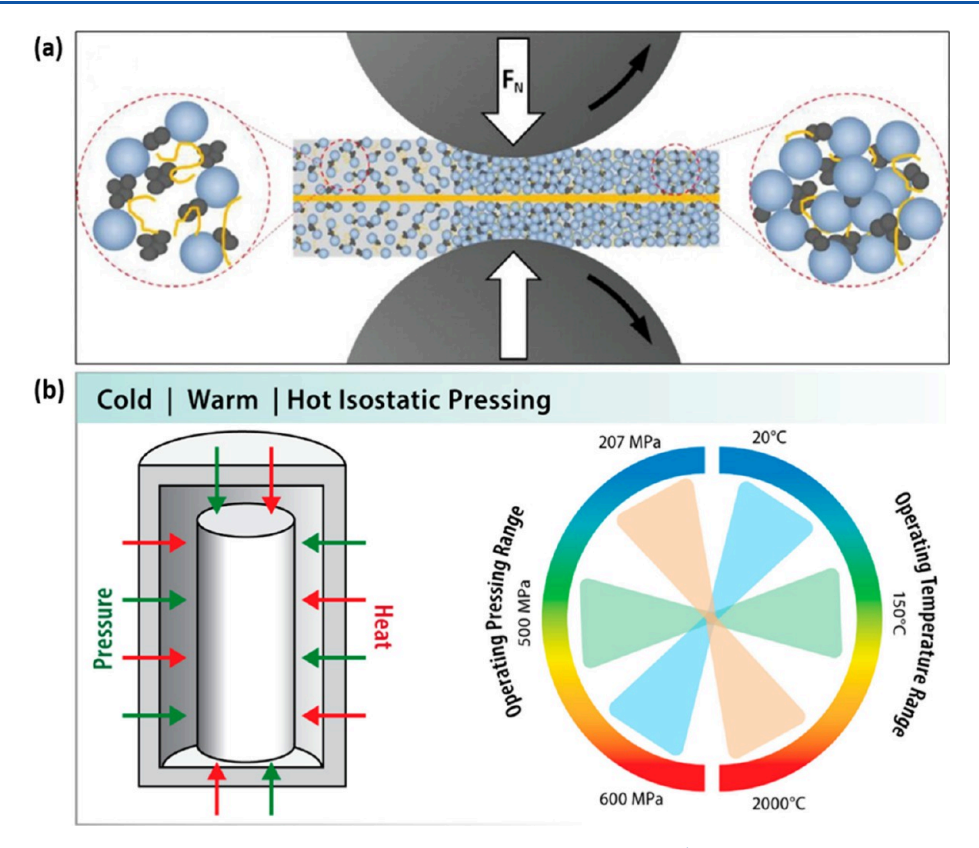


Figure 9. (a) Schematic illustration of the calendering process. Reproduced with permission. ¹⁰⁶ Copyright 2025, Elsevier. (b) Schematic diagram of a pressure vessel cavity into which the sample is inserted and subjected to isostatic pressure and temperature conditions, and temperature and pressure ranges for CIP (blue), WIP (green), and HIP (orange) techniques. Reproduced with permission. ¹⁰⁷ Copyright 2022 American Chemical Society.

conductivity decreased slightly. 102 Dry film processing is particularly effective for fabricating thick films, while it is less suitable for producing ultrathin layers. In contrast, solution processing is easier for creating thin films but poses challenges in achieving uniform thick coatings. Using PTFE as a binder for dry film fabrication, SE membranes with a thickness as thin as $18~\mu m$ have been reported. 103

PTFE has exceptional chemical stability against acids, bases, and solvents, along with high thermal resistance. However, it readily decomposes upon contact with lithium metal. The reduction reaction propagates through the fibrillated PTFE network, forming an electron-conductive carbon species. Such conductive pathways trigger an internal short circuit and obstruct ion conduction, ultimately destroying the safety and performance of the battery. For this reason, when PTFE is used in SE membranes, an additional protective treatment on the anode side may be required to ensure chemical compatibility.

4.4.2. Thermocompression. The thermocompression process is a method for producing a dense electrolyte membrane by compressing SE powder with thermoplastic polymer binders under high temperature and pressure (Figure 8b). This approach effectively reduces porosity in the SE membrane and improves ion conductivity. By utilizing polymeric binders with low melting or softening points, hot pressing at around 100 °C allows the viscous binder phase to flow between SE powders, filling voids and forming a continuous percolated SE network. 104 Without a binder, the hot-pressed Li₆PS₅Cl pellet will be prone to breakage. In contrast, the incorporation of a polyamide binder and applying thermal compression at 140 °C under 5 MPa yields a self-standing, flexible sulfide film. 104 Hot pressing also provides improved interfacial contacts between particles compared to cold pressing. 105 Through thermocompression of dry films, freestanding SE membranes with a thickness of 40 μm have been reported.

Despite offering benefits such as solvent-free manufacturing and a broader range of binder options compared with PTFE fibrillation-based methods, hot pressing requires a more complex thermocompression setup. More critically, it demands the use of specially designed molds for membrane shaping, which adds to the manufacturing complexity and cost. In addition, excessive polymer coverage around SE particles persists as a challenge in this approach, potentially hindering the ionic conductivity.

4.5. Pressurization Techniques. In addition to the fabrication strategies for SE membranes, controlling internal pores and defects within the SE membrane and ensuring strong adhesion of the electrode/electrolyte interface are also essential for the performance and reliability of ASSBs. To improve interfacial contact and densification, various pressurization processes are necessary following the formation of the SE membrane and electrode stacking. Among them, calendering 106 and WIP 107 are widely used (Figure 9).

Calendering is a traditional pressing process in which the electrode or SE film is passed between two rollers under constant pressure to achieve uniform thickness. ¹⁰⁸ This process planarizes the surface, improves thickness uniformity and particle bonding, and reduces porosity. Key process parameters include the line load, roll speed, and roll temperature. In particular, increasing the roll temperature reduces the required pressure and alleviates springback and interfacial shear stress. ¹⁰⁹ However, as it is a uniaxial compression method, calendering has limitations in applying even pressure distribution, especially in thick composites with rough surfaces.

WIP applies isotropic pressure to the entire sample using a fluid (mainly oil or water) as a pressure medium at temperatures below 150 °C. Moderately warm temperature is carefully chosen, not high enough to cause thermal degradation of electrode materials, yet sufficiently warm to promote effective interfacial contact. ¹¹⁰ Unlike the rigid roller-based calendering, the fluid in the WIP allows more meticulous pressure application. As a result, WIP has proven to be

highly effective in healing internal defects, achieving a dense SE membrane, and improving interfacial adhesion through superior compaction. In fact, it is very difficult to achieve reliably good electrochemical cycling in ASSBs without WIP at present. For instance, compared to uniaxial pressing, WIP has been shown to reduce porosity from 12% to 0.15% and, alongside notable improvements in membrane density, interfacial adhesion, and structural completion. In general, WIP for sulfide-based ASSBs is conducted within a pressure range of 400-600 MPa, most commonly around 490-500 MPa, at modest temperatures of 60-100 °C for several tens of minutes, depending on the materials and electrode stack design. 111-113 Despite the benefits, the WIP presents severe practical challenges. It requires huge space for bulky equipment, long preparation and processing times, and more complex operation procedures, making it difficult to implement at an industrial scale. Identifying a viable alternative to WIP is one of the most pressing challenges for the commercialization of ASSBs. This calls for the development of either advanced calendering techniques or entirely new, scalable pressurization approaches that retain the benefits of WIP while improving the manufacturability.

5. CONCLUSION

The development of sulfide-based SE membranes is a key factor for the realization of high-performance all-solid-state batteries (ASSBs). Sulfide electrolytes provide excellent ion conductivity and mechanical ductility, enabling low-temperature processing and facilitating the formation of close interfaces with electrodes. However, the chemical instability in air and limited electrochemical stability remain important challenges to overcome. To solve this problem, material-level strategies such as composition control to improve moisture stability and surface modification to stabilize electrochemical interfaces are actively underway.

Beyond materials, scalable and reliable fabrication methods are essential to bridge laboratory discoveries and industrial applications. Solution casting remains a versatile method for thin film fabrication, but it is constrained by solvent and binder compatibility. In contrast, dry processing approaches, such as PTFE fibrillation and thermocompression, have emerged as promising alternatives for producing dense, defect-free SE membranes with robust mechanical properties. At present, free-standing SE membranes prepared by solution casting, PTFE fibrillation, scaffold-based methods, or their combination could be the most feasible options. Once the relevant technologies mature, fabrication techniques could be expanded to solution casting via double casting, which offers particular advantages for producing ultrathin membranes with intimate electrode-electrolyte contact. However, as double casting may cause partial mixing between precast electrodes and the newly cast solution, careful optimization of processing conditions will be required. In addition, postfabrication pressurization techniques, including calendering and WIP, further enhance membrane densification and interfacial adhesion, both of which are critical to long-term battery performance.

In the future, the integration of ultrathin, mechanically reinforced sulfide SE membranes with optimized processing protocols will be key to realizing ASSBs with high energy density, cycling stability, and manufacturability. A multidisciplinary effort combining materials design, interface engineering, and process innovation is required to accelerate the commercialization of next-generation solid-state battery technology.

ASSOCIATED CONTENT

5 Supporting Information

The Supporting Information is available free of charge at https://pubs.acs.org/doi/10.1021/acsaem.5c02250.

Table of input parameters used to calculated estimated gravimetric and volumetric energy densities for various cell configurations (PDF)

AUTHOR INFORMATION

Corresponding Authors

Jinhan Cho — Department of Chemical and Biological Engineering, Korea University, Seoul 02841, Republic of Korea; ○ orcid.org/0000-0002-7097-5968; Email: jinhan71@korea.ac.kr

Jieun Lee − Energy Storage Research Center, Korea Institute of Science and Technology (KIST), Seoul 02792, Republic of Korea; orcid.org/0000-0003-4227-4125; Email: jieunlee23@kist.re.kr

Authors

Subin Kim – Energy Storage Research Center, Korea Institute of Science and Technology (KIST), Seoul 02792, Republic of Korea

Chaeyeon Shin — Energy Storage Research Center, Korea Institute of Science and Technology (KIST), Seoul 02792, Republic of Korea; Department of Chemical and Biological Engineering, Korea University, Seoul 02841, Republic of Korea

Complete contact information is available at: https://pubs.acs.org/10.1021/acsaem.5c02250

Author Contributions

§S. K. and C. S. contributed equally to this work.

Notes

The authors declare no competing financial interest.

ACKNOWLEDGMENTS

This research was supported by the National Research Council of Science & Technology (NST) grant by the Korea government (MSIT) (No. GTL24012-000) and the National Research Foundation of Korea (NRF) grant funded by the Ministry of Science and ICT of the Korea government (No. RS-2024-00451691).

■ REFERENCES

- (1) Janek, J.; Zeier, W. G. A Solid Future for Battery Development. *Nat. Energy* **2016**, *1* (9), 16141.
- (2) Tan, D. H. S.; Meng, Y. S.; Jang, J. Scaling up High-Energy-Density Sulfidic Solid-State Batteries: A Lab-to-Pilot Perspective. *Joule* **2022**, *6* (8), 1755–1769.
- (3) Hu, Y.-S. Batteries: Getting Solid. Nat. Energy 2016, 1 (4), 16042.
- (4) Li, Y.; Song, S.; Kim, H.; Nomoto, K.; Kim, H.; Sun, X.; Hori, S.; Suzuki, K.; Matsui, N.; Hirayama, M.; Mizoguchi, T.; Saito, T.; Kamiyama, T.; Kanno, R. A Lithium Superionic Conductor for Millimeter-Thick Battery Electrode. *Science* **2023**, *381* (6653), 50–53.
- (5) Zhou, L.; Zuo, T.-T.; Kwok, C. Y.; Kim, S. Y.; Assoud, A.; Zhang, Q.; Janek, J.; Nazar, L. F. High Areal Capacity, Long Cycle Life 4 V Ceramic All-Solid-State Li-Ion Batteries Enabled by Chloride Solid Electrolytes. *Nat. Energy* **2022**, *7* (1), 83–93.
- (6) Wang, K.; Ren, Q.; Gu, Z.; Duan, C.; Wang, J.; Zhu, F.; Fu, Y.; Hao, J.; Zhu, J.; He, L.; Wang, C.-W.; Lu, Y.; Ma, J.; Ma, C. A Cost-

- Effective and Humidity-Tolerant Chloride Solid Electrolyte for Lithium Batteries. *Nat. Commun.* **2021**, *12* (1), 4410.
- (7) Lee, J.; Lee, T.; Char, K.; Kim, K. J.; Choi, J. W. Issues and Advances in Scaling up Sulfide-Based All-Solid-State Batteries. *Acc. Chem. Res.* **2021**, 54 (17), 3390–3402.
- (8) Wang, C.; Kim, J. T.; Wang, C.; Sun, X. Progress and Prospects of Inorganic Solid-State Electrolyte-Based All-Solid-State Pouch Cells. *Adv. Mater.* **2023**, *35* (19), No. 2209074.
- (9) Tan, D. H. S.; Banerjee, A.; Chen, Z.; Meng, Y. S. From Nanoscale Interface Characterization to Sustainable Energy Storage Using All-Solid-State Batteries. *Nat. Nanotechnol.* **2020**, *15* (3), 170–180.
- (10) Lee, J.; Lee, K.; Lee, T.; Kim, H.; Kim, K.; Cho, W.; Coskun, A.; Char, K.; Choi, J. W. In Situ Deprotection of Polymeric Binders for Solution-Processible Sulfide-Based All-Solid-State Batteries. *Adv. Mater.* **2020**, 32 (37), No. 2001702.
- (11) Nikodimos, Y.; Ihrig, M.; Taklu, B. W.; Su, W.-N.; Hwang, B. J. Solvent-Free Fabrication of Freestanding Inorganic Solid Electrolyte Membranes: Challenges, Progress, and Perspectives. *Energy Storage Mater.* **2023**, *63*, No. 103030.
- (12) Kim, D. H.; Lee, Y.-H.; Song, Y. B.; Kwak, H.; Lee, S.-Y.; Jung, Y. S. Thin and Flexible Solid Electrolyte Membranes with Ultrahigh Thermal Stability Derived from Solution-Processable Li Argyrodites for All-Solid-State Li-Ion Batteries. *ACS Energy Lett.* **2020**, *5* (3), 718–727.
- (13) Cao, D.; Zhao, Y.; Sun, X.; Natan, A.; Wang, Y.; Xiang, P.; Wang, W.; Zhu, H. Processing Strategies to Improve Cell-Level Energy Density of Metal Sulfide Electrolyte-Based All-Solid-State Li Metal Batteries and Beyond. *ACS Energy Lett.* **2020**, 5 (11), 3468–3489
- (14) Monroe, C.; Newman, J. The Impact of Elastic Deformation on Deposition Kinetics at Lithium/Polymer Interfaces. *J. Electrochem. Soc.* **2005**, *152* (2), A396.
- (15) Rosner, M.; Cangaz, S.; Dupuy, A.; Hippauf, F.; Dörfler, S.; Abendroth, T.; Schumm, B.; Althues, H.; Kaskel, S. Toward Higher Energy Density All-Solid-State Batteries by Production of Freestanding Thin Solid Sulfidic Electrolyte Membranes in a Roll-to-Roll Process. *Adv. Energy Mater.* **2025**, *15* (19), No. 2404790.
- (16) Wu, J.; Yuan, L.; Zhang, W.; Li, Z.; Xie, X.; Huang, Y. Reducing the Thickness of Solid-State Electrolyte Membranes for High-Energy Lithium Batteries. *Energy Environ. Sci.* **2021**, *14* (1), 12–36.
- (17) Li, S.; Yang, Z.; Wang, S.-B.; Ye, M.; He, H.; Zhang, X.; Nan, C.-W.; Wang, S. Sulfide-Based Composite Solid Electrolyte Films for All-Solid-State Batteries. *Commun. Mater.* **2024**, *5* (1), 44.
- (18) Liu, H.; Liang, Y.; Wang, C.; Li, D.; Yan, X.; Nan, C.-W.; Fan, L.-Z. Priority and Prospect of Sulfide-Based Solid-Electrolyte Membrane. *Adv. Mater.* **2023**, *35* (50), No. 2206013.
- (19) Zhang, D.; Xu, X.; Qin, Y.; Ji, S.; Huo, Y.; Wang, Z.; Liu, Z.; Shen, J.; Liu, J. Recent Progress in Organic-Inorganic Composite Solid Electrolytes for All-Solid-State Lithium Batteries. *Chem.—Eur. J.* **2020**, *26* (8), 1720–1736.
- (20) Dixit, M.; Parejiya, A.; Essehli, R.; Muralidharan, N.; Haq, S. U.; Amin, R.; Belharouak, I. SolidPAC Is an Interactive Battery-on-Demand Energy Density Estimator for Solid-State Batteries. *Cell Rep. Phys. Sci.* **2022**, 3 (2), No. 100756.
- (21) Zhang, N.; Zhao, X.; Liu, G.; Peng, Z.; Wu, J.; Men, M.; Yao, X. Solid Electrolyte Membranes for All-Solid-State Rechargeable Batteries. *eTransportation* **2024**, *20*, No. 100319.
- (22) Song, Y. B.; Baeck, K. H.; Kwak, H.; Lim, H.; Jung, Y. S. Dimensional Strategies for Bridging the Research Gap between Lab-Scale and Potentially Practical All-Solid-State Batteries: The Role of Sulfide Solid Electrolyte Films. *Adv. Energy Mater.* **2023**, *13* (32), No. 2301142.
- (23) Heubner, C.; Maletti, S.; Auer, H.; Hüttl, J.; Voigt, K.; Lohrberg, O.; Nikolowski, K.; Partsch, M.; Michaelis, A. From Lithium-Metal toward Anode-Free Solid-State Batteries: Current Developments, Issues, and Challenges. *Adv. Funct. Mater.* **2021**, *31* (51), No. 2106608.

- (24) Lee, J.; Zhao, C.; Wang, C.; Chen, A.; Sun, X.; Amine, K.; Xu, G.-L. Bridging the Gap between Academic Research and Industrial Development in Advanced All-Solid-State Lithium-Sulfur Batteries. *Chem. Soc. Rev.* **2024**, *53* (10), 5264–5290.
- (25) Lim, H.-D.; Park, J.-H.; Shin, H.-J.; Jeong, J.; Kim, J. T.; Nam, K.-W.; Jung, H.-G.; Chung, K. Y. A Review of Challenges and Issues Concerning Interfaces for All-Solid-State Batteries. *Energy Storage Mater.* **2020**, *25*, 224–250.
- (26) Zhang, Q.; Cao, D.; Ma, Y.; Natan, A.; Aurora, P.; Zhu, H. Sulfide-Based Solid-State Electrolytes: Synthesis, Stability, and Potential for All-Solid-State Batteries. *Adv. Mater.* **2019**, *31* (44), No. 1901131.
- (27) Ribes, M.; Barrau, B.; Souquet, J. L. Sulfide Glasses: Glass Forming Region, Structure and Ionic Conduction of Glasses in Na_2S - XS_2 (X= Si; Ge), Na_2S - P_2S_5 and Li_2S -GeS $_2$ Systems. J. Non-Cryst. Solids 1980, 38–39, 271–276.
- (28) Dietrich, C.; Weber, D. A.; Sedlmaier, S. J.; Indris, S.; Culver, S. P.; Walter, D.; Janek, J.; Zeier, W. G. Lithium Ion Conductivity in Li₂S-P₂S₅ Glasses Building Units and Local Structure Evolution during the Crystallization of Superionic Conductors Li₃PS₄, Li₇P₃S₁₁ and L. *J. Mater. Chem. A* **2017**, *5* (34), 18111–18119.
- (29) Warren, Z.; Rosero-Navarro, N. C. Solution-Based Suspension Synthesis of Li₂S-P₂S₅ Glass-Ceramic Systems as Solid-State Electrolytes: A Brief Review of Current Research. *ACS Omega* **2024**, *9* (29), 31228–31236.
- (30) Mercier, R.; Malugani, J. P.; Fahys, B.; Douglande, J.; Robert, G. Synthese, Structure Cristalline et Analyse Vibrationnelle de l'hexathiohypodiphosphate de Lithium Li₄P₂S₆. *J. Solid State Chem.* **1982**, 43 (2), 151–162.
- (31) Homma, K.; Yonemura, M.; Kobayashi, T.; Nagao, M.; Hirayama, M.; Kanno, R. Crystal Structure and Phase Transitions of the Lithium Ionic Conductor Li₃PS₄. *Solid State Ionics* **2011**, *182* (1), 53–58.
- (32) Kong, S. T.; Gün, Ö.; Koch, B.; Deiseroth, H. J.; Eckert, H.; Reiner, C. Structural Characterisation of the Li Argyrodites Li₇PS₆ and Li₇PSe₆ and Their Solid Solutions: Quantification of Site Preferences by MAS-NMR Spectroscopy. *Chem.–Eur. J.* **2010**, *16* (17), 5138–5147.
- (33) Kudu, Ö. U.; Famprikis, T.; Fleutot, B.; Braida, M.-D.; Le Mercier, T.; Islam, M. S.; Masquelier, C. A Review of Structural Properties and Synthesis Methods of Solid Electrolyte Materials in the Li,S-P₂S₅ Binary System. *J. Power Sources* **2018**, 407, 31–43.
- (34) Mizuno, F.; Hayashi, A.; Tadanaga, K.; Tatsumisago, M. High Lithium Ion Conducting Glass-Ceramics in the System Li₂S-P₂S₅. *Solid State Ionics* **2006**, *177* (26), *2721*–2725.
- (35) Deiseroth, H.-J.; Kong, S.-T.; Eckert, H.; Vannahme, J.; Reiner, C.; Zaiß, T.; Schlosser, M. Li₆PS₅X: A Class of Crystalline Li-Rich Solids With an Unusually High Li⁺ Mobility. *Angew. Chem., Int. Ed.* **2008**, *47* (4), 755–758.
- (36) Hanghofer, I.; Gadermaier, B.; Wilkening, H. M. R. Fast Rotational Dynamics in argyrodite-Type Li6PSSX (X: Cl, Br, I) as Seen by 31P Nuclear Magnetic Relaxation—On Cation-Anion Coupled Transport in Thiophosphates. *Chem. Mater.* **2019**, 31 (12), 4591–4597.
- (37) Kanno, R.; Murayama, M. Lithium Ionic Conductor Thio-LISICON: The Li₂S GeS₂ P₂S₅ System. *J. Electrochem. Soc.* **2001**, *148* (7), A742.
- (38) Murayama, M.; Kanno, R.; Kawamoto, Y.; Kamiyama, T. Structure of the Thio-LISICON, Li₄GeS₄. *Solid State Ionics* **2002**, 154–155, 789–794.
- (39) Kato, Y.; Hori, S.; Kanno, R. Li₁₀GeP₂S₁₂-Type Superionic Conductors: Synthesis, Structure, and Ionic Transportation. Adv. Energy Mater. **2020**, 10 (42), No. 2002153.
- (40) Geller, S. The crystal structure of y Ag8GeTe6, a potential mixed electronic-ionic conductor. *Z. Für Krist. Cryst. Mater.* **1979**, 149 (1–4), 31–47.
- (41) Feng, X.; Chien, P.-H.; Wang, Y.; Patel, S.; Wang, P.; Liu, H.; Immediato-Scuotto, M.; Hu, Y.-Y. Enhanced Ion Conduction by

- Enforcing Structural Disorder in Li-Deficient Argyrodites Li_{6-x}PS_{5-x}Cl_{1+x}. Energy Storage Mater. **2020**, 30, 67–73.
- (42) Wang, H.; Gao, L.; Lu, Z.; Tang, Y.; Ye, D.; Zhao, G.; Zhao, H.; Zhang, J. Borohydride Substitution Effects of Li₆PS₅Cl Solid Electrolyte. *ACS Appl. Energy Mater.* **2021**, *4* (11), 12079–12083.
- (43) Guo, H.; Li, J.; Burton, M.; Cattermull, J.; Liang, Y.; Chart, Y.; Rees, G. J.; Aspinall, J.; Pasta, M. High-Entropy Sulfide argyrodite Electrolytes for All-Solid-State Lithium-Sulfur Batteries. *Cell Rep. Phys. Sci.* **2024**, *5* (10), No. 102228.
- (44) Kamaya, N.; Homma, K.; Yamakawa, Y.; Hirayama, M.; Kanno, R.; Yonemura, M.; Kamiyama, T.; Kato, Y.; Hama, S.; Kawamoto, K.; Mitsui, A. A Lithium Superionic Conductor. *Nat. Mater.* **2011**, *10* (9), 682–686
- (45) Kim, M.; Seo, J.; Suba, J. P. D.; Cho, K. Y. A Review of Polymers in Sulfide-Based Hybrid Solid-State Electrolytes for All-Solid-State Lithium Batteries. *Mater. Chem. Front.* **2023**, 7 (22), 5475–5499.
- (46) Hayashi, A.; Hama, S.; Morimoto, H.; Tatsumisago, M.; Minami, T. Preparation of $\text{Li}_2\text{S}-\text{P}_2\text{S}_5$ Amorphous Solid Electrolytes by Mechanical Milling. *J. Am. Ceram. Soc.* **2001**, 84 (2), 477–479.
- (47) Seino, Y.; Ota, T.; Takada, K.; Hayashi, A.; Tatsumisago, M. A Sulphide Lithium Super Ion Conductor Is Superior to Liquid Ion Conductors for Use in Rechargeable Batteries. *Energy Environ. Sci.* **2014**, 7 (2), 627–631.
- (48) Rao, R. P.; Adams, S. Studies of Lithium argyrodite Solid Electrolytes for All-Solid-State Batteries. *Phys. Status Solidi A* **2011**, 208 (8), 1804–1807.
- (49) Kanno, R.; Hata, T.; Kawamoto, Y.; Irie, M. Synthesis of a New Lithium Ionic Conductor, Thio-LISICON-Lithium Germanium Sulfide System. *Solid State Ionics* **2000**, *130* (1), 97–104.
- (50) Kaib, T.; Haddadpour, S.; Andersen, H. F.; Mayrhofer, L.; Järvi, T. T.; Moseler, M.; Möller, K.-C.; Dehnen, S. Quaternary Diamond-Like Chalcogenidometalate Networks as Efficient Anode Material in Lithium-Ion Batteries. *Adv. Funct. Mater.* **2013**, 23 (46), 5693–5699.
- (51) Bron, P.; Johansson, S.; Zick, K.; Schmedt auf der Günne, J.; Dehnen, S.; Roling, B. Li10SnP2S12: An Affordable Lithium Superionic Conductor. J. Am. Chem. Soc. 2013, 135 (42), 15694–15697.
- (52) Whiteley, J. M.; Woo, J. H.; Hu, E.; Nam, K.-W.; Lee, S.-H. Empowering the Lithium Metal Battery through a Silicon-Based Superionic Conductor. *J. Electrochem. Soc.* **2014**, *161* (12), A1812.
- (53) Deng, Z.; Wang, Z.; Chu, I.-H.; Luo, J.; Ong, S. P. Elastic Properties of Alkali Superionic Conductor Electrolytes from First Principles Calculations. *J. Electrochem. Soc.* **2016**, *163* (2), A67.
- (54) Kato, A.; Nose, M.; Yamamoto, M.; Sakuda, A.; Hayashi, A.; Tatsumisago, M. Mechanical Properties of Sulfide Glasses in All-Solid-State Batteries. *J. Ceram. Soc. Jpn.* **2018**, 126 (9), 719–727.
- (55) Yadav, N. G.; Folastre, N.; Bolmont, M.; Jamali, A.; Morcrette, M.; Davoisne, C. Study of Failure Modes in Two Sulphide-Based Solid Electrolyte All-Solid-State Batteries via in Situ SEM. *J. Mater. Chem. A* **2022**, *10* (33), 17142–17155.
- (56) Liang, J.; Li, X.; Wang, C.; Kim, J. T.; Yang, R.; Wang, J.; Sun, X. Current Status and Future Directions in Environmental Stability of Sulfide Solid-State Electrolytes for All-Solid-State Batteries. *Energy Mater. Adv.* **2023**, *4*, No. 0021.
- (57) Chen, Y.-T.; Marple, M. A. T.; Tan, D. H. S.; Ham, S.-Y.; Sayahpour, B.; Li, W.-K.; Yang, H.; Lee, J. B.; Hah, H. J.; Wu, E. A.; Doux, J.-M.; Jang, J.; Ridley, P.; Cronk, A.; Deysher, G.; Chen, Z.; Meng, Y. S. Investigating Dry Room Compatibility of Sulfide Solid-State Electrolytes for Scalable Manufacturing. *J. Mater. Chem. A* **2022**, *10* (13), 7155–7164.
- (58) Sahu, G.; Lin, Z.; Li, J.; Liu, Z.; Dudney, N.; Liang, C. Air-Stable, High-Conduction Solid Electrolytes of Arsenic-Substituted Li₄SnS₄. *Energy Environ. Sci.* **2014**, *7* (3), 1053–1058.
- (59) Hyun, S.; Tao, W.; Ko, J.; Han, B. Elucidation of Degradation Mechanism of a Li-argyrodite Solid Electrolyte against Moisture and Proposal of Design Principles for Robust Stability. *Cell Rep. Phys. Sci.* **2025**, *6* (5), No. 102600.

- (60) Sun, Y.; Suzuki, K.; Hara, K.; Hori, S.; Yano, T.; Hara, M.; Hirayama, M.; Kanno, R. Oxygen Substitution Effects in $\text{Li}_{10}\text{GeP}_2\text{S}_{12}$ Solid Electrolyte. *J. Power Sources* **2016**, 324, 798–803.
- (61) Hayashi, A.; Muramatsu, H.; Ohtomo, T.; Hama, S.; Tatsumisago, M. Improvement of Chemical Stability of Li3PS4 Glass Electrolytes by Adding M_xO_y (M = Fe, Zn, and Bi) Nanoparticles. *J. Mater. Chem. A* **2013**, *1* (21), 6320–6326.
- (62) Nikodimos, Y.; Huang, C.-J.; Taklu, B. W.; Su, W.-N.; Hwang, B. J. Chemical Stability of Sulfide Solid-State Electrolytes: Stability toward Humid Air and Compatibility with Solvents and Binders. *Energy Environ. Sci.* **2022**, *15* (3), 991–1033.
- (63) Zhu, Y.; He, X.; Mo, Y. Origin of Outstanding Stability in the Lithium Solid Electrolyte Materials: Insights from Thermodynamic Analyses Based on First-Principles Calculations. ACS Appl. Mater. Interfaces 2015, 7 (42), 23685–23693.
- (64) Tan, D. H. S.; Wu, E. A.; Nguyen, H.; Chen, Z.; Marple, M. A. T.; Doux, J.-M.; Wang, X.; Yang, H.; Banerjee, A.; Meng, Y. S. Elucidating Reversible Electrochemical Redox of Li₆PS₅Cl Solid Electrolyte. *ACS Energy Lett.* **2019**, *4* (10), 2418–2427.
- (65) Wenzel, S.; Randau, S.; Leichtweiß, T.; Weber, D. A.; Sann, J.; Zeier, W. G.; Janek, J. Direct Observation of the Interfacial Instability of the Fast Ionic Conductor Li₁₀GeP₂S₁₂ at the Lithium Metal Anode. *Chem. Mater.* **2016**, 28 (7), 2400–2407.
- (66) Wang, C.; Wang, C.; Li, M.; Zhang, S.; Zhang, C.; Chou, S.; Mao, J.; Guo, Z. Design of Thin Solid-State Electrolyte Films for Safe and Energy-Dense Batteries. *Mater. Today* **2024**, *72*, 235–254.
- (67) Zhang, X.; Wang, Q. J.; Harrison, K. L.; Roberts, S. A.; Harris, S. J. Pressure-Driven Interface Evolution in Solid-State Lithium Metal Batteries. *Cell Rep. Phys. Sci.* **2020**, *1* (2), No. 100012.
- (68) Ning, Z.; Jolly, D. S.; Li, G.; De Meyere, R.; Pu, S. D.; Chen, Y.; Kasemchainan, J.; Ihli, J.; Gong, C.; Liu, B.; Melvin, D. L. R.; Bonnin, A.; Magdysyuk, O.; Adamson, P.; Hartley, G. O.; Monroe, C. W.; Marrow, T. J.; Bruce, P. G. Visualizing Plating-Induced Cracking in Lithium-Anode Solid-Electrolyte Cells. *Nat. Mater.* **2021**, *20* (8), 1121–1129.
- (69) Schnell, J.; Tietz, F.; Singer, C.; Hofer, A.; Billot, N.; Reinhart, G. Prospects of Production Technologies and Manufacturing Costs of Oxide-Based All-Solid-State Lithium Batteries. *Energy Environ. Sci.* **2019**, *12*, 1818–1833.
- (70) Liang, J.; Luo, J.; Sun, Q.; Yang, X.; Li, R.; Sun, X. Recent Progress on Solid-State Hybrid Electrolytes for Solid-State Lithium Batteries. *Energy Storage Mater.* **2019**, *21*, 308–334.
- (71) Hippauf, F.; Schumm, B.; Doerfler, S.; Althues, H.; Fujiki, S.; Shiratsuchi, T.; Tsujimura, T.; Aihara, Y.; Kaskel, S. Overcoming Binder Limitations of Sheet-Type Solid-State Cathodes Using a Solvent-Free Dry-Film Approach. *Energy Storage Mater.* **2019**, *21*, 390–398.
- (72) Emley, B.; Liang, Y.; Chen, R.; Wu, C.; Pan, M.; Fan, Z.; Yao, Y. On the Quality of Tape-Cast Thin Films of Sulfide Electrolytes for Solid-State Batteries. *Mater. Today Phys.* **2021**, *18*, No. 100397.
- (73) Chen, X.; He, W.; Ding, L.-X.; Wang, S.; Wang, H. Enhancing Interfacial Contact in All Solid State Batteries with a Cathode-Supported Solid Electrolyte Membrane Framework. *Energy Environ. Sci.* **2019**, *12* (3), 938–944.
- (74) Oh, J.; Choi, S. H.; Kim, H.; Chung, W. J.; Kim, M.; Kim, I.; Lee, T.; Lee, J.; Kim, D. O.; Moon, S.; Kim, D.; Choi, J. W. Solvent-Binder Engineering for a Practically Viable Solution Process for Fabricating Sulfide-Based All-Solid-State Batteries. *ACS Energy Lett.* **2025**, *10* (6), 2831–2838.
- (75) Zhao, X.; Shen, L.; Zhang, N.; Yang, J.; Liu, G.; Wu, J.; Yao, X. Stable Binder Boosting Sulfide Solid Electrolyte Thin Membrane for All-Solid-State Lithium Batteries. *Energy Mater. Adv.* **2024**, *S*, No. 0074.
- (76) Emley, B.; Wu, C.; Zhao, L.; Ai, Q.; Liang, Y.; Chen, Z.; Guo, L.; Terlier, T.; Lou, J.; Fan, Z.; Yao, Y. Impact of Fabrication Methods on Binder Distribution and Charge Transport in Composite Cathodes of All-Solid-State Batteries. *Mater. Futures* **2023**, *2* (4), No. 045102.
- (77) Singer, C.; Schmalzbauer, S.; Daub, R. Influence of the Slurry Composition on Thin-Film Components for the Wet Coating Process

- of Sulfide-Based All-Solid-State Batteries. J. Energy Storage 2023, 68, No. 107703.
- (78) Mills, A.; Yang, G.; Tsai, W.-Y.; Chen, X. C.; Sacci, R. L.; Armstrong, B. L.; Hallinan, D. T.; Nanda, J. Adverse Effects of Trace Non-Polar Binder on Ion Transport in Free-Standing Sulfide Solid Electrolyte Separators. *J. Electrochem. Soc.* **2023**, *170* (8), No. 080513.
- (79) Tan, D. H. S.; Banerjee, A.; Deng, Z.; Wu, E. A.; Nguyen, H.; Doux, J.-M.; Wang, X.; Cheng, J.; Ong, S. P.; Meng, Y. S.; Chen, Z. Enabling Thin and Flexible Solid-State Composite Electrolytes by the Scalable Solution Process. ACS Appl. Energy Mater. 2019, 2 (9), 6542–6550.
- (80) Choi, J.; Bak, C.; Kim, J. Y.; Shin, D. O.; Kang, S. H.; Lee, Y. M.; Lee, Y.-G. Enhancing Electrochemo-Mechanical Properties of Graphite-Silicon Anode in All-Solid-State Batteries via Solvent-Induced Polar Interactions in Nitrile Binders. *J. Energy Chem.* **2025**, 105, 514–524.
- (81) Lee, K.; Lee, J.; Choi, S.; Char, K.; Choi, J. W. Thiol-Ene Click Reaction for Fine Polarity Tuning of Polymeric Binders in Solution-Processed All-Solid-State Batteries. ACS Energy Lett. 2019, 4 (1), 94–101.
- (82) Lee, K.; Kim, S.; Park, J.; Park, S. H.; Coskun, A.; Jung, D. S.; Cho, W.; Choi, J. W. Selection of Binder and Solvent for Solution-Processed All-Solid-State Battery. *J. Electrochem. Soc.* **2017**, *164* (9), A2075.
- (83) Yamamoto, M.; Terauchi, Y.; Sakuda, A.; Takahashi, M. Binder-Free Sheet-Type All-Solid-State Batteries with Enhanced Rate Capabilities and High Energy Densities. Sci. Rep. 2018, 8 (1), 1212.
- (84) Kim, K. T.; Kwon, T. Y.; Jung, Y. S. Scalable Fabrication of Sheet-Type Electrodes for Practical All-Solid-State Batteries Employing Sulfide Solid Electrolytes. *Curr. Opin. Electrochem.* **2022**, *34*, No. 101026.
- (85) Lee, J.; Choi, J. W. Block Copolymer Binders with Hard and Soft Segments for Scalable Fabrication of Sulfide-Based All-Solid-State Batteries. *EcoMat* **2022**, *4* (4), No. e12193.
- (86) Inada, T.; Takada, K.; Kajiyama, A.; Kouguchi, M.; Sasaki, H.; Kondo, S.; Watanabe, M.; Murayama, M.; Kanno, R. Fabrications and Properties of Composite Solid-State Electrolytes. *Solid State Ionics* **2003**, *158* (3), *275*–280.
- (87) Nam, Y. J.; Oh, D. Y.; Jung, S. H.; Jung, Y. S. Toward Practical All-Solid-State Lithium-Ion Batteries with High Energy Density and Safety: Comparative Study for Electrodes Fabricated by Dry- and Slurry-Mixing Processes. *J. Power Sources* **2018**, *375*, 93–101.
- (88) Hong, S.-B.; Jang, Y.-R.; Jung, Y.-C.; Cho, W.; Kim, D.-W. Sulfide-Based Flexible Solid Electrolyte Enhancing Cycling Performance of All-Solid-State Lithium Batteries. *ACS Appl. Energy Mater.* **2024**, *7* (12), 5193–5201.
- (89) Cao, D.; Li, Q.; Sun, X.; Wang, Y.; Zhao, X.; Cakmak, E.; Liang, W.; Anderson, A.; Ozcan, S.; Zhu, H. Amphipathic Binder Integrating Ultrathin and Highly Ion-Conductive Sulfide Membrane for Cell-Level High-Energy-Density All-Solid-State Batteries. *Adv. Mater.* **2021**, 33 (52), No. 2105505.
- (90) Zhang, Y.; Chen, R.; Wang, S.; Liu, T.; Xu, B.; Zhang, X.; Wang, X.; Shen, Y.; Lin, Y.-H.; Li, M.; Fan, L.-Z.; Li, L.; Nan, C.-W. Free-Standing Sulfide/Polymer Composite Solid Electrolyte Membranes with High Conductance for All-Solid-State Lithium Batteries. *Energy Storage Mater.* **2020**, *25*, 145–153.
- (91) Oh, D. Y.; Nam, Y. J.; Park, K. H.; Jung, S. H.; Cho, S.-J.; Kim, Y. K.; Lee, Y.-G.; Lee, S.-Y.; Jung, Y. S. Excellent Compatibility of Solvate Ionic Liquids with Sulfide Solid Electrolytes: Toward Favorable Ionic Contacts in Bulk-Type All-Solid-State Lithium-Ion Batteries. *Adv. Energy Mater.* **2015**, *5* (22), No. 1500865.
- (92) Oh, D. Y.; Nam, Y. J.; Park, K. H.; Jung, S. H.; Kim, K. T.; Ha, A. R.; Jung, Y. S. Slurry-Fabricable Li⁺-Conductive Polymeric Binders for Practical All-Solid-State Lithium-Ion Batteries Enabled by Solvate Ionic Liquids. *Adv. Energy Mater.* **2019**, *9* (16), No. 1802927.
- (93) Liu, S.; Zhou, L.; Han, J.; Wen, K.; Guan, S.; Xue, C.; Zhang, Z.; Xu, B.; Lin, Y.; Shen, Y.; Li, L.; Nan, C.-W. Super Long-Cycling All-Solid-State Battery with Thin Li₆PS₃Cl-Based Electrolyte. *Adv. Energy Mater.* **2022**, *12* (25), No. 2200660.

- (94) Nam, Y. J.; Cho, S.-J.; Oh, D. Y.; Lim, J.-M.; Kim, S. Y.; Song, J. H.; Lee, Y.-G.; Lee, S.-Y.; Jung, Y. S. Bendable and Thin Sulfide Solid Electrolyte Film: A New Electrolyte Opportunity for Free-Standing and Stackable High-Energy All-Solid-State Lithium-Ion Batteries. *Nano Lett.* **2015**, *15* (5), 3317–3323.
- (95) El-Shinawi, H.; Darnbrough, E.; Perera, J.; McClelland, I.; Armstrong, D. E. J.; Cussen, E. J.; Cussen, S. A. Liquid-Phase Approach to Glass-Microfiber-Reinforced Sulfide Solid Electrolytes for All-Solid-State Batteries. *ACS Appl. Mater. Interfaces* **2023**, *15* (30), 36512–36518.
- (96) Zhu, G.-L.; Zhao, C.-Z.; Peng, H.-J.; Yuan, H.; Hu, J.-K.; Nan, H.-X.; Lu, Y.; Liu, X.-Y.; Huang, J.-Q.; He, C.; Zhang, J.; Zhang, Q. A Self-Limited Free-Standing Sulfide Electrolyte Thin Film for All-Solid-State Lithium Metal Batteries. *Adv. Funct. Mater.* **2021**, *31* (32), No. 2101985.
- (97) Guo, R.; Zhang, K.; Zhao, W.; Hu, Z.; Li, S.; Zhong, Y.; Yang, R.; Wang, X.; Wang, J.; Wu, C.; Bai, Y. Interfacial Challenges and Strategies toward Practical Sulfide-Based Solid-State Lithium Batteries. *Energy Mater. Adv.* **2023**, *4*, No. 0022.
- (98) Liu, J.; Lin, H.; Li, H.; Zhao, D.; Liu, W.; Tao, X. In Situ Polymerization Derived from PAN-Based Porous Membrane Realizing Double-Stabilized Interface and High Ionic Conductivity for Lithium-Metal Batteries. ACS Appl. Mater. Interfaces 2024, 16 (16), 21264–21272.
- (99) Liu, M.; Hong, J. J.; Sebti, E.; Zhou, K.; Wang, S.; Feng, S.; Pennebaker, T.; Hui, Z.; Miao, Q.; Lu, E.; Harpak, N.; Yu, S.; Zhou, J.; Oh, J. W.; Song, M.-S.; Luo, J.; Clément, R. J.; Liu, P. Surface Molecular Engineering to Enable Processing of Sulfide Solid Electrolytes in Humid Ambient Air. *Nat. Commun.* 2025, 16 (1), 213. (100) Wang, X.; Chen, S.; Zhang, K.; Huang, L.; Shen, H.; Chen, Z.; Rong, C.; Wang, G.; Jiang, Z. A Polytetrafluoroethylene-Based Solvent-Free Procedure for the Manufacturing of Lithium-Ion Batteries. *Materials* 2023, 16 (22), 7232.
- (101) Lee, D.; Shim, Y.; Kim, Y.; Kwon, G.; Choi, S. H.; Kim, K.; Yoo, D.-J. Shear Force Effect of the Dry Process on Cathode Contact Coverage in All-Solid-State Batteries. *Nat. Commun.* **2024**, *15* (1), 4763.
- (102) Lee, D. J.; Jang, J.; Lee, J.-P.; Wu, J.; Chen, Y.-T.; Holoubek, J.; Yu, K.; Ham, S.-Y.; Jeon, Y.; Kim, T.-H.; Lee, J. B.; Song, M.-S.; Meng, Y. S.; Chen, Z. Physio-Electrochemically Durable Dry-Processed Solid-State Electrolyte Films for All-Solid-State Batteries. *Adv. Funct. Mater.* **2023**, 33 (28), No. 2301341.
- (103) Yoon, S.; Kang, S. H.; Choi, J.; Kim, J. Y.; Lee, Y.-G.; Park, Y.-S.; Shin, D. O. Regulating Entanglement Networks of Fibrillatable Binders for Sub-20- μ m Thick, Robust, Dry-Processed Solid Electrolyte Membranes in All-Solid-State Batteries. *Small* **2025**, *21* (13), No. 2407882.
- (104) Hu, L.; Ren, Y.; Wang, C.; Li, J.; Wang, Z.; Sun, F.; Ju, J.; Ma, J.; Han, P.; Dong, S.; Cui, G. Fusion Bonding Technique for Solvent-Free Fabrication of All-Solid-State Battery with Ultrathin Sulfide Electrolyte. *Adv. Mater.* **2024**, *36* (29), No. 2401909.
- (105) Lee, S.-E.; Sim, H.-T.; Lee, Y.-J.; Hong, S.-B.; Chung, K. Y.; Jung, H.-G.; Kim, D.-W. Li₆PS₅Cl-Based Composite Electrolyte Reinforced with High-Strength Polyester Fibers for All-Solid-State Lithium Batteries. *J. Power Sources* **2022**, *542*, No. 231777.
- (106) Chen, J.; Asachi, M.; Hassanpour, A.; Babaie, M.; Jabbari, M. Modelling of Lithium-Ion Battery Electrode calendering: A Critical Review. *J. Energy Storage* **2025**, *123*, No. 116702.
- (107) Dixit, M.; Beamer, C.; Amin, R.; Shipley, J.; Eklund, R.; Muralidharan, N.; Lindqvist, L.; Fritz, A.; Essehli, R.; Balasubramanian, M.; Belharouak, I. The Role of Isostatic Pressing in Large-Scale Production of Solid-State Batteries. *ACS Energy Lett.* **2022**, *7* (11), 3936–3946.
- (108) Abdollahifar, M.; Cavers, H.; Scheffler, S.; Diener, A.; Lippke, M.; Kwade, A. Insights into Influencing Electrode calendering on the Battery Performance. *Adv. Energy Mater.* **2023**, *13* (40), No. 2300973. (109) Meyer, C.; Weyhe, M.; Haselrieder, W.; Kwade, A. Heated calendering of Cathodes for Lithium-Ion Batteries with Varied

- Carbon Black and Binder Contents. Energy Technol. 2020, 8 (2), No. 1900175.
- (110) Attia, U. M. Cold-Isostatic Pressing of Metal Powders: A Review of the Technology and Recent Developments. *Crit. Rev. Solid State Mater. Sci.* **2021**, 46 (6), 587–610.
- (111) Hiraoka, K.; Sakabe, J.; Suzuki, N.; Seki, S. Operando and Ex Situ Raman Spectroscopies for Evaluating Carbon Structural Changes in Anode-Free-Type Sulfide-Based All-Solid-State Li-Ion Batteries. *J. Mater. Chem. A* **2025**, *13* (34), 27960–27969.
- (112) Choi, S. H.; Baek, C. H.; Oh, J.; Lee, G.-J.; Kim, M.; Lee, H.; Yoo, D.-J.; Jung, Y. S.; Kim, K.; Yu, J.-S.; Cho, W.; Park, H.; Choi, J. W. Silver Exsolution from Li-argyrodite Electrolytes for Initially Anode-Free All-Solid-State Batteries. *Nat. Commun.* **2025**, *16* (1), 5871.
- (113) Lee, Y.-G.; Fujiki, S.; Jung, C.; Suzuki, N.; Yashiro, N.; Omoda, R.; Ko, D.-S.; Shiratsuchi, T.; Sugimoto, T.; Ryu, S.; Ku, J. H.; Watanabe, T.; Park, Y.; Aihara, Y.; Im, D.; Han, I. T. High-Energy Long-Cycling All-Solid-State Lithium Metal Batteries Enabled by Silver-Carbon Composite Anodes. *Nat. Energy* **2020**, *5* (4), 299–308.